

**INTER-AMERICAN TROPICAL TUNA COMMISSION**

**SCIENTIFIC ADVISORY COMMITTEE**

**SEVENTH MEETING**

**La Jolla, California (USA)**

**09-13 May 2016**

**DOCUMENT SAC-07-05a**

**STATUS OF BIGEYE TUNA IN THE EASTERN PACIFIC OCEAN IN 2015 AND OUTLOOK  
FOR THE FUTURE**

Alexandre Aires-da-Silva, Carolina Minte-Vera and Mark N. Maunder

**CONTENTS**

|   |    |
|---|----|
| Executive summary.....  | 2  |
| 1. Introduction .....   | 3  |
| 2. Data .....   | 3  |
| 2.1. Changes in bigeye size-composition data from Japanese longline fisheries ..... | 4  |
| 3. Model structure configurations .....   | 4  |
| 4. Results .....  | 6  |
| 4.1. Base case model.....   | 6  |
| 4.1.1. Recruitment and biomass.....   | 6  |
| 4.1.2. Fishing mortality ( $F$ ).....   | 7  |
| 4.1.3. Model diagnostics.....   | 7  |
| 4.2. Sensitivity analyses.....  | 9  |
| 4.2.1. Steepness.....   | 9  |
| 4.2.2. Data weighting.....  | 9  |
| 4.2.3. Growth.....  | 9  |
| 4.2.4. Juvenile natural mortality.....  | 10 |
| 4.2.5. Adult natural mortality .....  | 10 |
| 4.3. Management quantities.....   | 10 |
| 4.3.1. Base case model .....  | 10 |
| 4.3.2. Sensitivity to alternative model configurations .....                        | 11 |
| 5. Future directions .....  | 11 |
| Acknowledgements.....   | 12 |
| References .....  | 12 |
| Appendices .....  | 24 |

## **EXECUTIVE SUMMARY**

1. The assessment of bigeye tuna in the eastern Pacific Ocean in 2015 is similar to the previous assessment, except that separate series of length-frequency data for Japanese longline commercial and training vessels are now available, and both were used in the assessment.
2. The results of this assessment indicate a recovering trend for bigeye in the EPO during 2005-2009, subsequent to IATTC tuna conservation resolutions initiated in 2004. However, although the resolutions have continued since 2009, the rebuilding trend was not sustained during 2010-2012, and the spawning biomass ratio (SBR) gradually declined to a historically low level of 0.16 at the start of 2013. This decline may be related to a series of recent below-average recruitments which coincided with a series of strong La Niña events. More recently, the SBR is estimated to have increased slightly, from 0.16 in 2013 to 0.20 at the start of 2016; in the model, this increase is driven mainly by the recent increase in the catch per unit of effort (CPUE) of the longline fisheries that catch adult bigeye. There is uncertainty about recent and future levels of recruitment and biomass. At current levels of fishing mortality ( $F$ ), and if recent levels of effort and catchability continue and recruitment remains average, the spawning biomass ( $S$ ) is predicted to continue rebuilding and stabilize at about 0.22, above the level corresponding to the maximum sustainable yield (MSY) (0.21).
3. The recent fishing mortality rates are estimated to be below the level corresponding to MSY, whereas recent spawning biomasses are estimated to be slightly below that level. These interpretations are uncertain and highly sensitive to the assumptions made about the steepness parameter ( $h$ ) of the stock-recruitment relationship, the weighting assigned to the size-composition data (in particular to the longline size-composition data), the growth curve, and the assumed rates of natural mortality ( $M$ ) for bigeye.
4. The following topics should be a priority in future research into the bigeye stock assessment:
  - a. Investigation of the causes of model misspecification responsible for the two-regime recruitment pattern in the bigeye assessment (average length of the oldest fish in the model ( $L_2$ ), natural mortality, others).
  - b. Formulation of a growth curve that is more representative of the data.
  - c. Weighting of the different data sets.
  - d. Fishery definitions.
  - e. Stock structure. The IATTC staff will continue collaborating with the Secretariat of the Pacific Community (SPC) on a Pacific-wide assessment of bigeye. This will incorporate new tagging data in a spatially-structured population dynamics model, which will help to evaluate potential biases resulting from the current approach of conducting separate assessments for the EPO and the Western and Central Pacific Ocean (WCPO).

## **1. INTRODUCTION**

This report presents the most current stock assessment of bigeye tuna (*Thunnus obesus*) in the eastern Pacific Ocean (EPO). An integrated statistical age-structured stock assessment model (Stock Synthesis 3.23b) was used in the assessment. During 2015, the IATTC staff worked in collaboration with Japanese scientists to improve the size-composition data for bigeye caught by the Japanese longline fisheries. As a result, the major improvement in this assessment consists of changes in these data and how they are used in the model.

Bigeye tuna are distributed across the Pacific Ocean, but the bulk of the catch is made to the east and to the west. The purse-seine catches of bigeye are substantially lower close to the western boundary of the EPO (150°W); the longline catches are more continuous, but relatively low between 160°W and 180°. Bigeye are not often caught by purse seiners in the EPO north of 10°N, but a substantial portion of the longline catches of bigeye in the EPO is taken north of that parallel. The assessment is conducted as if there were a single stock of bigeye in the EPO, with minimal net movement of fish between the EPO and the western and central Pacific Ocean (WCPO). The results are consistent with those of other Pacific-wide analyses of bigeye. However, a large amount of conventional and electronic tagging data has recently become available from the Pacific Tuna Tagging Programme, which has focused its tagging efforts between 180° and 140°W since 2008 (Schaefer *et al.* 2015). The tag recoveries clearly show that there is extensive longitudinal movement of bigeye across the IATTC's management boundary at 150°W, in particular from west to east. The staff of the Secretariat of the Pacific Community (SPC) constructed a Pacific-wide stock assessment model to test the sensitivity of management advice for the WCPO to the assumption that dynamics of bigeye in the EPO can effectively be ignored when conducting WCPO stock assessments (McKechnie *et al.* 2015). The results indicated that the dynamics of bigeye in the WCPO estimated by the Pacific-wide model are not substantially different from those estimated by the WCPO-only model, and that it is therefore reasonable to continue to make management recommendations to the Western and Central Pacific Fisheries Commission (WCPFC) on the basis of WCPO regional assessment models. A major modeling challenge that is recognized in the Pacific-wide bigeye research is possible misspecification in the model from assuming common growth across the Pacific when available studies indicate regional differences. With respect to the EPO, the IATTC staff will continue to collaborate with SPC on the Pacific-wide assessment for bigeye. This will incorporate the new tagging data in a spatially-structured population dynamics model, which will help in the ongoing evaluation of potential biases resulting from ignoring exchange of fish across the WCPO-EPO boundary in the current approach of conducting separate assessments for the EPO and WCPO.

## **2. DATA**

The stock assessment requires a substantial amount of information. Data on retained catch, discards, catch per unit of effort (CPUE), and size compositions of the catches from several different fisheries have been analyzed. Several assumptions regarding processes such as growth, recruitment, movement, natural mortality ( $M$ ), and fishing mortality ( $F$ ), have also been made. Catch and CPUE data for the surface fisheries have been updated, and include new data for 2015. New or updated longline catch data are available for China (2014), Japan (2013-2014), Korea (2006, 2014), Chinese Taipei (2012-2014), the United States (2013-2014), French Polynesia (2013-2014), Vanuatu (2007-2014) and other nations (2013-2015). Longline catch data for 2015 are available for China, Japan, Chinese Taipei, and Korea from the monthly report statistics. For longline fisheries with no new catch data for 2015, catches were assumed to be the same as in 2014. New or updated CPUE data are available for the Japanese longline fleet for the entire assessment period (1975-2015). Japan has re-submitted its catch and effort (including hooks-per-basket information) data, to contain only commercial data (previously there was a mix of commercial and training vessel data). New purse-seine length-frequency data are available for 2015. New Japanese longline length-

frequency data are also available, as described below.

### **2.1. Changes in bigeye size-composition data from Japanese longline fisheries**

Previous stock assessments of bigeye in the EPO have noted a prominent residual pattern in the model fit to the length composition of the longline fisheries. The pattern consisted of a major shift from positive residuals (observations larger than model predictions) for medium-size fish prior to the late 1980s, to a period of positive residuals for larger fish thereafter ([Aires-da-Silva et al. 2010](#)). Several hypotheses have been proposed to explain this residual pattern: one is that it is caused by a major change in the methodology for collecting and processing the size-composition data (e.g. different length conversion factors, or length-weight relationships).

During 2015, IATTC staff worked closely with Japanese fishery scientists to investigate the possible causes of the residual pattern (Satoh *et al.* 2015). The conclusion of this collaborative study was that the pattern appeared to be caused by a combination of converting raw weight measurements of gilled-and-gutted fish to fork length and combining the size-composition data for the commercial fleets and training vessels. As a result of this study, new or updated length-frequency data are available for the Japanese commercial longline fleet (1986-2014). The length-frequency data are now available for commercial vessels and training vessels separately, and by measurement type (weight or length) (Satoh *et al.* 2016) for the entire assessment period (1975-2014). Weight-frequency data for the commercial longline fleet are also available, but they are not used in the assessment due to uncertainty in the weight conversion factors. A detailed description of these newly-submitted data and recommendations for their best use in the bigeye and yellowfin assessments is provided by Minte-Vera *et al.* (2016).

### **3. MODEL STRUCTURE CONFIGURATIONS**

With a few exceptions, described below, the base case model used in this bigeye assessment is the same as that used in the previous full assessment, conducted in 2014 ([IATTC Stock Assessment Report 15](#)). That base case included several improvements. First, a new Richards growth curve, estimated externally from an integrated analysis of otolith-based age data and tag-recapture observations, was introduced (Aires-da-Silva *et al.* 2015). This new growth curve reduced the uncertainty about the average size of the oldest fish ( $L_2$  parameter); also, the parameters that determine the variance of the length-at-age were taken from the new externally-derived growth estimates.

Following a recommendation by the [external review of the bigeye assessment](#), two time blocks (early and late fisheries, split at 1990, associated with the size-composition residual pattern) with different catchability parameters had been assumed for all longline fisheries. As described above (section 2.1), the residual pattern in the longline size-composition data found in previous assessments is likely to be artificial. Therefore, the time blocks for the longline fisheries are no longer justified, and it is recommended that they be eliminated from the model (Minte-Vera *et al.* 2016). The Japanese longline CPUE should be treated as a continuous series of indices of abundance, with no splits in catchability. This would reduce the number of fisheries defined in the bigeye stock assessment from 23 to 19 (Table 1). The spatial extent of each fishery and the boundaries of the length-frequency sampling areas are shown in Figure 1. They are defined on the basis of gear type (purse seine, pole-and-line, and longline), purse-seine set type (on floating objects, unassociated schools, and dolphins), time period, IATTC length-frequency sampling area or latitude, and unit of longline catch (in numbers or weight). The length-composition data for the Japanese training vessels and the weight-composition data for the Japanese commercial vessels (not used in the model fit but included for comparative purposes), are included in the model as "surveys<sup>1</sup>", not fisheries (Minte-Vera *et al.* 2016).

---

<sup>1</sup> Stock Synthesis terminology; does not represent actual surveys, but allows flexibility in how data is modelled.

Also related to the assumption of early and late time-blocks of catchability, split at 1990, for the longline fisheries, in the previous full assessment the same time-blocks were assumed for the selectivity of these fisheries ([IATTC Stock Assessment Report 15](#)). That assessment assumed dome-shaped selectivities for the early period of the Central and Southern longline fisheries (Fisheries 13 and 14) and logistic selectivity for their later period. Since these time blocks were eliminated in the current assessment, logistic selectivities are assumed for the whole history of both these fisheries, in which the largest sizes of bigeye are observed.

As in the previous assessment, the number of CPUE data series used as indices of abundance was reduced, in order to minimize conflicting trends among data sets. A reduced set of indices of abundance for the Central and Southern longline fisheries (Fisheries 13 and 14) was chosen to best represent the bigeye stock trends.

Diagnostic analyses with the [previous base case model configuration](#) indicated a dominant influence of the size-composition data (mainly from the longline fisheries) in determining the productivity ( $R_0$  parameter) of the bigeye stock, and conflicts among datasets were also found. This could be at least partially caused by the prominent residual pattern in the longline size-composition data (see section 2.1). In order to minimize these issues, these size-composition data were down-weighted for all fisheries in the previous full assessment ([IATTC Stock Assessment Report 15](#)).

One of the expected outcomes of resolving the inconsistencies in the Japanese longline size-composition data (section 2.1.) was to allow these data to be up-weighted, to better inform the model about cohort strength and longline size selectivity. Unfortunately, doing so did not eliminate the dominant influence of the size-composition data in determining the productivity of the stock ( $R_0$ , see section 4.1.3b), which is not desirable in statistical stock assessment models (Francis 2011). In addition to this shortcoming, up-weighting the composition data brought back the previous “two-regime” recruitment pattern which had been mostly resolved in the previous full assessment ([IATTC Stock Assessment Report 15](#)). This may be due to some existing model mis-specification (e.g. growth, natural mortality), and more research needs to be conducted to investigate this problem. However, as long as the model mis-specification is not resolved, in this assessment the weighting of the size-composition data assumed in the previous full assessment is used. Analyses of sensitivity to alternative weightings and biological processes which may be contributing to the model mis-specification were carried out (see Appendices).

The important aspects of the base case assessment (1) and the five sensitivity analyses (2-6) are as follows:

1. **Base case assessment:** steepness ( $h$ ) of the stock-recruitment relationship = 1 (no relationship between stock and recruitment); fixed mean length-at-age, and fixed parameters that define the variability of the length-at-age; fitted to CPUE time series for Fisheries 13 and 14 (Central and Southern longline; asymptotic size-based selectivities for Fisheries 13 and 14, which catch larger bigeye; and down-weighted the size-composition data for all fisheries (a multiplicative weighting factor –  $\lambda$  (lambda) - of 0.05 was applied to all size-composition data, as in the previous full assessment: [IATTC Stock Assessment Report 15](#)).
2. **Sensitivity to the steepness of the stock-recruitment relationship.** The base case assessment assumes that recruitment is independent of stock size ( $h = 1$ ); the sensitivity analysis included a Beverton-Holt (1957) stock-recruitment relationship with a steepness of  $h = 0.75$ .
3. **Sensitivity to weighting assigned to the size-composition data.** As noted above, in the base case model,  $\lambda = 0.05$  was applied to the size-composition data of all surface and longline fisheries. The following sensitivity analyses were done to explore the effect on the assessment results of assigning different weights to individual fisheries or groups of fisheries: 1) up-weighting the size-composition

data of all fisheries to their original weighting ( $\lambda = 1$ ); 2) up-weighting to  $\lambda = 1$  the size-composition data for all fisheries except Fisheries 13 and 14 (Central and Southern longline), for which  $\lambda = 0.2$  and  $0.1$ , respectively, as indicated by a likelihood profile on  $R_0$  (see section 4.1.3b).

4. **Sensitivity to lower values of the average size of the oldest fish ( $L_2$ )**. The base case assumes  $L_2$  fixed at 196 cm, a value that is taken from the Richards growth curve estimated externally from an integrated analysis of otolith-based age -data and tag-recapture observations (Aires-da-Silva *et al.* 2015). This study was updated, using the Francis (2015) method, to include three additional tag-recovery records for bigeye, all with times at liberty greater than 10 years ([Figure D.1](#)). A sensitivity analysis was run using the new estimate of  $L_2$  from the updated integrated model (193 cm). A second sensitivity analysis considered an even lower  $L_2$  of 183 cm. A closer inspection of the growth model fit ([Figure D.1](#)) revealed negative residuals for all of the oldest fish (>8 years old), which suggests that a more flexible model may be needed that can bend over faster towards a lower  $L_2$ . Inspection of the empirical tag-recovery data indicated a lower  $L_2$  (at about 183 cm) than was estimated from fitting the Richards growth model. Therefore, the second sensitivity assumed the  $L_2$  of 183 cm. The  $L_2$  sensitivity runs were done for two data-weighting configurations of the length-composition data ( $\lambda = 0.05$  for all fisheries, as in the base case, and using the original sample sizes for all fisheries,  $\lambda = 1$ ).
5. **Sensitivity to assuming higher values of juvenile natural mortality ( $M$ ) for both females and males**. A sensitivity analysis for juvenile  $M$  investigated the effect of variations in the shape of the young segment of the  $M$  schedules assumed for males and females ([Figure E.1](#)). The sensitivity analyses were conducted by assuming one of two different levels of  $M$  for age-0 fish (0.25 and 0.50 quarter-1), and a linear decreasing trend of  $M$  between age-0 and one of three possible young ages (5, 10 and 13 quarters). The juvenile  $M$  sensitivity analyses were done for two data-weighting configurations of the length-composition data ( $\lambda = 0.05$  for all fisheries, as in the base case, and using the original sample sizes for all fisheries,  $\lambda = 1$ ).
6. **Sensitivity to assuming lower and higher values of adult natural mortality ( $M$ ) for both females and males**. While defining the alternative adult  $M$  schedules for bigeye, and in order to maintain the age-specific absolute differences of  $M$  estimated from sex-ratio data, the  $M$  values for adult (12+ quarters old) females and males assumed in the base case were decreased or increased by the same multiplicative factor ([Figure F.1](#)). The adult  $M$  sensitivity analyses were done for two data-weighting configurations of the length-composition data ( $\lambda = 0.05$  for all fisheries, as in the base case, and using the original sample sizes for all fisheries,  $\lambda = 1$ ).

## 4. RESULTS

### 4.1. Base case model

#### 4.1.1. Recruitment and biomass

A prominent feature in the time series of estimated bigeye recruitment is that the highest recruitment peaks of 1983 and 1998 coincide with the strongest El Niño events during the historic period of the assessment ([Figure 2](#)). There was a period of above-average annual recruitment during 1994-1998, followed by a period of below-average recruitment in 1999-2000. The recruitments were above average from 2001 to 2006, and were particularly strong in 2005. More recently, the recruitments were below average during 2007-2009, but above average during 2010-2015. The most recent (2015) annual recruitment is estimated to be above average. The El Niño event in 2015 was stronger than those of 1983 and 1998. Given that the highest historic peaks in recruitment coincided with those El Niño events, recruitment can be expected to be high in 2015. The model did not estimate this high recruitment in 2015, but there are few data for 2015 in the model to inform the estimate. The 2015 estimate is highly uncertain and should be regarded with caution, because recently-recruited bigeye are represented in only

a few length-frequency data sets.

Over the range of spawning biomasses estimated by the base case assessment, the abundance of bigeye recruits appears to be unrelated to the spawning potential of adult females at the time of hatching.

Since the start of 2005, the spawning biomass ratio (SBR; the ratio of the spawning biomass at that time to that of the unfished stock) has gradually increased, to 0.26 at the start of 2009. This may be attributed to the combined effect of a series of above-average recruitments since 2001, the IATTC tuna conservation resolutions, and decreased longline fishing effort in the EPO during 2004-2008. However, although the resolutions have continued since 2009, the rebuilding trend was not sustained during 2010-2013, and the SBR gradually declined to a historically low level of 0.16 at the start of 2013 ([Figure 3](#)). This decline could be related to a period dominated by below-average recruitments that began in 2007 and coincides with a series of particularly strong La Niña events. More recently, the SBR is estimated to have increased slightly, from 0.16 in 2013 to 0.20 at the start of 2016; in the model, this increase is driven mainly by the recent increase in the CPUE of the longline fisheries that catch adult bigeye.

#### **4.1.2. Fishing mortality ( $F$ )**

There have been important changes in the amount of fishing mortality caused by the fisheries that catch bigeye in the EPO. On average, since 1993 the fishing mortality of bigeye less than about 15 quarters old has increased substantially, but has fallen in recent years. For fish more than about 15 quarters old,  $F$  also increased initially, but then fluctuated around a constant level ([Figure 4](#)). The increase in the fishing mortality of the younger fish was caused by the expansion of the purse-seine fisheries that catch tuna in association with floating objects. It is clear that the longline fishery had the greatest impact on the stock prior to 1995, but with the decrease in longline effort and the expansion of the floating-object fishery, at present the impact of the purse-seine fishery on the bigeye stock is far greater than that of the longline fishery ([Figure 5](#)). The discarding of small bigeye has a small, but detectable, impact on the depletion of the stock.

#### **4.1.3. Model diagnostics**

##### **4.1.3.a Model fit**

In general, the base case model fits very well to the indices of abundance of the Central and Southern longline fisheries (13 and 14) ([Figure A.1a](#)). As might be expected because the composition data are down-weighted, the base case does not fit the composition data well. The Stock Synthesis assessment model produces an extensive series of model fit diagnostics. These are available for the base case model in [html](#) and [pdf](#) formats.

##### **4.1.3.b $R_0$ profile**

Likelihood profiling of virgin recruitment, a method for diagnosing over-weighting of size-composition data, data conflicts, and model misspecification, was applied to the bigeye tuna assessment. Virgin recruitment ( $R_0$ ; the equilibrium recruitment in the absence of fishing) is a common parameter in stock assessment that scales the population size. Information on population size comes from two main sources: 1) how catch changes indices of relative abundance; and 2) how the relative abundance changes in consecutive ages of age-composition data (or appropriately adjusted size-composition data). Francis (2011) argues that abundance information should primarily come from indices of abundance, and not from composition data. The diagnostic indicates over-weighting of composition data or model misspecification when the composition component of the likelihood profile for  $R_0$  provides substantial information about  $R_0$  and conflicts with information from the relative abundance index data. The model misspecification should be corrected (e.g. the selectivity curve for the fishery or survey related to those composition data should be modified) or the weighting of the composition data reduced, so that the

composition data have little information on  $R_0$ .

As a result of the changes in the size-composition data of the Japanese longline fisheries (see section 2.1), the weighting of the different datasets in the bigeye assessment model needed re-evaluation. For this purpose, an  $R_0$  profile was constructed using the base case modified by keeping the original weighting ( $\lambda = 1$ ) for the size-composition data of all fisheries. One important aspect is revealed by the  $R_0$  likelihood profile diagnostic (Figure C.1). The  $R_0$  maximum likelihood estimate at about 8.5 (in log space) is strongly driven by the dominant gradient provided by the size-composition data of Fisheries 13 and 14 (Central and Southern longline), for which logistic selectivity is assumed. The change in the negative log-likelihood for these fisheries is about 30 and 90 units higher, respectively, compared to that of other data components. This diagnostic is indicative of over-weighting of composition data and/or some form of model misspecification that will have to be addressed in the future in order to allocate the proper weighting of datasets in the bigeye model. As in the previous full assessment ([IATTC Stock Assessment Report 15](#)), a multiplicative weighting factor of 0.05 was applied equally to all size-composition data in the base case.

#### 4.1.3.c Age-structured production diagnostic

The age-structured production model (ASPM) diagnostic was proposed by Maunder and Piner (2015) as a way to: (i) further evaluate model misspecification, (ii) ascertain the influence of composition data on the estimates of absolute abundance and trends in abundance, and (iii) check whether catch alone can explain the trends in the indices of abundance. The ASPM diagnostic is computed as follows: (i) run the base case model; (ii) fix selectivity parameters at the maximum likelihood estimates (MLE) from the base case model, (iii) turn off the estimation of all parameters except the scaling parameters, and set the recruitment deviates to zero; (iv) fit the model to the indices of abundance only; (v) compare the estimated trajectory to the one obtained in the base case. If the ASPM is able to fit the indices of abundance that have good contrast (e.g. those that have declining and/or increasing trends) well, Maunder and Piner (2015) suggest that this is evidence of the existence of a production function, and the indices will likely provide information about absolute abundance. They refer to this situation as “the catch explains the indices well”; in the opposite case, where there is no good fit to the indices, “the catch cannot explain the indices”. This can have several causes: (i) the stock is recruitment-driven; (ii) the stock has not yet declined to the point where catch is a major factor influencing abundance, (iii) the base-case model is incorrect, or (iv) the indices of relative abundance are not proportional to abundance. Checking whether the stock is recruitment-driven involves simply fitting the ASPM with the recruitment deviates fixed at the values estimated in the base case. If this still does not capture the population trajectory estimated in the integrated model, it can be concluded that the information about scale in the integrated model is coming from the composition data. Large confidence intervals on the abundance estimated by the ASPM also indicate that the index of abundance has little information on absolute abundance.

The ASPM diagnostic fit to the indices of abundance shows a general decline over time, with a sharper decline in the mid-1990s when the purse seine fishery on floating objects expanded (Figure A.1b). This is the general trend of the indices of abundance, but the model is unable to fit the fluctuations in abundance caused by recruitment. As a result, the estimated trajectory of the spawning biomass does not reflect major fluctuations, except that caused by the expansion of the floating-object fisheries in the mid-1990s (Figure A.2). The confidence intervals are much smaller than for the base case.

When the recruitment deviates are estimated in the ASPM, the model is able to fit fluctuations in abundance caused by recruitment (Figure A.1c). In fact, the model fit to the CPUE data is nearly identical to that from the base case (Figure A.1a). However, the confidence intervals are much larger, indicating that most of the uncertainty in the assessment comes from fluctuations in recruitment rather than parameter estimation. Model structure uncertainty that is not included in the parameter estimation

uncertainty also adds substantially to the uncertainty in the stock assessment (see sensitivity analyses in the Appendices). The estimated SBR time series is very similar to base case estimates (Figure A.2). The same result is obtained for the ASPM with recruitment deviates fixed at the estimates from the base case. These results indicate that the abundance information, both absolute and relative, contained in the CPUE-based indices of relative abundance cannot be interpreted without accounting for the fluctuations in recruitment, and that the composition data are having little influence on the base case estimates of absolute abundance or trends in abundance.

## 4.2. Sensitivity analyses

The results of the four sensitivity analyses are presented in the appendices: sensitivity to (a) the stock-recruitment relationship (Appendix B); (b) assigning different weighting to the size-composition data (Appendix C); c) assuming lower values for the average size of the oldest fish,  $L_2$  (Appendix D); d) assuming higher rates of juvenile natural mortality ( $M$ ) (Appendix E); and, assuming lower and higher rates of adult natural mortality ( $M$ ) (Appendix F). Here we describe differences in model fit and model estimation, and defer our discussion of differences in stock status until Section 4.3.

### 4.2.1. Steepness

The steepness ( $h$ ) of the Beverton-Holt (1957) stock-recruitment relationship was set at 0.75. The time series of relative recruitment is similar to that of the base case ([Figure B.1](#)). With respect to the spawning biomass, the relative trends in the SBR are very similar between the base case and the model that assumes a stock-recruitment relationship ([Figure B.2](#)).

### 4.2.2. Data weighting

As noted earlier, one of the expected outcomes of resolving the inconsistencies in the Japanese longline size-composition data (section 2.1) was to allow these data to be up-weighted, to better inform the model about cohort strength and size selectivity. Unfortunately, doing so did not eliminate the previous dominant influence of the size-composition data in determining the productivity of the stock ( $R_0$ , see section 4.1.3b), which is not desirable in statistical stock assessment models (Francis 2011). Up-weighting the composition data for all fisheries in the model ( $\lambda = 1$ ) brought back the previous “two-regime” recruitment pattern, which had already been mostly resolved in the previous full assessment ([Figure C.2](#)). This result is likely related to the persisting dominant influence of the size-composition data of the logistic-selectivity longline fisheries (Fisheries 13 and 14). In fact, when the composition data of only these fisheries are down-weighted, while retaining the original sample sizes of the composition data from other fisheries ( $\lambda = 0.2$  and  $0.3$  for Fisheries 13 and 14, and  $\lambda = 1$  for all other fisheries), the “two-regime” recruitment pattern is greatly minimized ([Figure C.2](#)). Some existing form of model mis-specification (e.g. growth, natural mortality) may be behind the dominant influence of the longline size-composition data. This mis-specification needs to be resolved before re-weighting the size composition data.

### 4.2.3. Growth

Sensitivity analyses were conducted assuming two lower values (193 and 183 cm) for the average size of the oldest fish ( $L_2$ ). When the size-composition data weighting applied in the base case ( $\lambda = 0.05$  for all fisheries) was used in the sensitivity analyses, lower values of  $L_2$  did not produce great differences in relative recruitment: even the lowest  $L_2$  value of 183 cm did not resolve the two-regime recruitment pattern ([Figure D.3a](#)). In contrast, lower values of  $L_2$  produced great differences in relative recruitment when the original sample sizes of the size composition data ( $\lambda = 1$ ) were applied to all fisheries. Using  $L_2$  of 196 cm, as in the base case, resulted in the two-regime recruitment pattern, indicating that there may still be some form of mis-specification in the model. In contrast, using a lower value of  $L_2$  reduced this pattern ([Figure D.3b](#)). This suggests that growth may be the source (or one of various sources) of the model mis-

specification that needs to be resolved in the bigeye assessment.

In terms of the spawning biomass, assuming a lower value of  $L_2$  results in more optimistic SBR levels. This is to be expected, given that the lower  $L_2$  implies that the model expects to find smaller proportions of the larger fish in the data, hence a less depleted stock. Using  $L_2$  of 196 cm, as in the base case, but keeping the original sample sizes of the composition data ( $\lambda = 0.05$ ), produced pessimistic estimates of the SBR. However, as noted above, the prominent two-regime recruitment pattern that this analysis produced indicates strong model mis-specification.

#### 4.2.4. Juvenile natural mortality

When the size-composition weighting used in the base case is applied ( $\lambda = 0.05$  for all fisheries), assuming higher rates of juvenile natural mortality ( $M$ ) does not improve the two-regime recruitment pattern ([Figure E.2a](#)) much. In contrast, it is improved when the original sample sizes of the size composition data are kept ( $\lambda = 1$ ) ([Figure E.2b](#)). However, these higher  $M$  levels need to be applied to a larger number of juvenile age-classes (scenario M5, for example) in order for the improvement to be noticeable. Such high levels of juvenile  $M$  may not be biologically reasonable.

#### 4.2.5. Adult natural mortality

As described in [Aires-da-Silva, Maunder and Tomlinson \(2010\)](#), assuming higher rates of adult  $M$  contributes to minimizing the “two-regime” recruitment pattern ([Figure F.2](#)). However, these rates (scenario 5, for example) seem unreasonably high for bigeye, possibly because the average length of the oldest fish is assumed to be high in the base case. These sensitivity analyses for lower  $L_2$  should be further explored to investigate the remaining source of model mis-specification in the assessment.

As expected, assuming higher values for adult  $M$  results in overly optimistic levels of spawning biomass. With higher  $M$  for adults, the model has to generate higher levels of recruitment in order to explain the observed catches.

### 4.3. Management quantities

#### 4.3.1. Base case model

According to the base case results, at the beginning of 2016 the spawning biomass ( $S$ ) of bigeye in the EPO was about 4% below  $S_{MSY}$ , and the recent catches are estimated to have been about 3% lower than the MSY. If fishing mortality ( $F$ ) is proportional to fishing effort, and the current patterns of age-specific selectivity are maintained,  $F_{MSY}$  is about 5% higher than the current level of effort ([Table 1](#)).

According to the base case results, the most recent estimate indicates that the bigeye stock in the EPO is slightly overfished ( $S < S_{MSY}$ ) and that overfishing is not taking place ( $F < F_{MSY}$ ) ([Figure 6](#)). Likewise, the current base case model indicates that the interim limit reference points of  $0.38 S_{MSY}$  and  $1.6 F_{MSY}$ , which correspond to a 50% reduction in recruitment from its average unexploited level based on a conservative value for the steepness ( $h = 0.75$ ) of the Beverton-Holt stock-recruitment relationship, have not been exceeded ([Figure 6](#)). These interpretations, however, are subject to uncertainty, as indicated by the approximate confidence intervals around the most recent estimate in the phase plots ([Figure 6](#)), but they do not exceed the limit reference points. Note that the confidence intervals consider only parameter estimation uncertainty, and do not include uncertainty in fixed parameters or model structure (see the sensitivity analyses for this type of uncertainty).

The MSY of bigeye in the EPO could be maximized if the age-specific selectivity pattern were similar to that of the longline fisheries, because they catch larger individuals that are close to the critical weight. Before the expansion of the floating-object purse-seine fishery that began in 1993, the MSY was greater than the current MSY, and the fishing mortality was much less than  $F_{MSY}$  ([Figure 7](#)).

At current levels of fishing mortality, and if recent levels of effort and catchability continue and recruitment remains at about average levels, the spawning biomass is predicted to continue rebuilding, and stabilize at an SBR of 0.22 around 2023, above the level corresponding to MSY (0.21) ([Figure 3](#)). If a stock-recruitment relationship is assumed, it is estimated that catches will be lower in the future at current levels of fishing effort, particularly for the surface fisheries ([Figure 8](#)).

These simulations are based on the assumption that selectivity and catchability patterns will not change in the future. Changes in targeting practices or increased catchability of bigeye as abundance declines (e.g. density-dependent catchability) could result in differences from the outcomes predicted here.

#### 4.3.2. Sensitivity to alternative model configurations

The interpretations of stock status are strongly dependent on the assumptions made about the steepness parameter ( $h$ ) of the stock-recruitment relationship, the weighting assigned to the size-composition data, the growth curve, and the assumed levels of juvenile and adult natural mortality ( $M$ ).

The sensitivity analysis that included a stock-recruitment relationship with  $h = 0.75$  estimated the SBR required to support the MSY to be 0.30, compared to 0.21 for the base case assessment (Table B.1). The sensitivity analysis for  $h = 0.75$  estimated an  $F$  multiplier of 0.91, considerably lower than that for the base case assessment (1.05). The base case model results indicate that the recent spawning biomass level is slightly below that corresponding to MSY ( $S_{\text{recent}}/S_{\text{MSY}} = 0.96$ ); this MSY-related depletion value is estimated to be lower (0.81) for the sensitivity analysis with  $h = 0.75$ .

The management quantities estimated in the stock assessment are highly sensitive to the weighting of the size-composition data ([Table C.1](#)). Using the original sample sizes for all fisheries ( $\lambda = 1$ ) in the model produces overly pessimistic management quantities ( $F$  multiplier = 0.57;  $S_{\text{recent}}/S_{\text{MSY}} = 0.41$ ). This is due to the dominance of the size-composition data of Fisheries 13 and 14 (which assume logistic selectivities) in determining absolute scale (the  $R_0$  parameter) in the model (see section 4.1.3b). This is indicative of over-weighting of composition data and/or some form of model misspecification that will have to be addressed in the future in order to assign the proper weighting of datasets in the bigeye model. Once this dominance is balanced out by down-weighting these data ( $\lambda = 0.2$  and 0.3 for Fisheries 13 and 14, respectively), other data components (mainly the longline CPUE) are allowed to also inform the model on absolute scale ( $R_0$ ). As a result, management quantities are less pessimistic.

Lowering the average size of the oldest fish produces a more optimistic stock status ([Table D.1](#)).

The effect on management quantities of assuming higher rates of juvenile natural mortality depends on the number of age classes to which those higher rates apply. The estimates of stock status become more optimistic if higher  $M$  values are applied to a larger number of juvenile age-classes. These increases are greater if the original length-composition sample sizes are maintained ( $\lambda = 1$ ) ([Table E.1](#)).

When lower rates of adult natural mortality are assumed for bigeye of both sexes, the estimate of stock status is more pessimistic than the base case (lower  $F$  multiplier) ([Table F.1](#)). Assuming higher adult natural mortality rates produces the opposite effect (higher  $F$  multiplier) ([Table F.1](#)). However, the highest rates considered in this sensitivity analysis seem biologically unrealistic for bigeye. Likewise, the  $S_{\text{recent}}/S_{\text{MSY}}$  ratio is highly sensitive to the assumed rates of adult natural mortality: specifically, it decreases and increases, respectively, with lower and higher assumed values of  $M$ .

## 5. FUTURE DIRECTIONS

The following topics should be a priority in future research into the bigeye stock assessment:

1. Investigation of the causes of model misspecification responsible for the two-regime recruitment pattern in the bigeye assessment (average length of the oldest bigeye in the model ( $L_2$ ), natural

- mortality, others)
2. Formulation of a growth curve that is more representative of the data
  3. Weighting of the different data sets
  4. Fishery definitions
  5. Stock structure (continuing collaboration with SPC staff on Pacific-wide bigeye stock assessments)

## **ACKNOWLEDGEMENTS**

Many IATTC and member country staff provided data for the assessment. Richard Deriso, IATTC staff members, and member country scientists provided advice on the stock assessment, fisheries, and biology of bigeye tuna. Christine Patnode provided assistance with the figures.

## **REFERENCES**

- Aires-da Silva, A. M., Maunder, M. N., Schaefer, K. M., and Fuller, D. W. (2015). Improved growth estimates from integrated analysis of direct aging and tag-recapture data: An illustration with bigeye tuna (*Thunnus obesus*) of the eastern pacific ocean with implications for management. *Fisheries Research*, 163:119-126.
- Francis, R.I.C. 2011. Data weighting in statistical fisheries stock assessment models. *Can. J. Fish. Aquat. Sci.* 68: 1124:1138.
- Francis, R.I.C., Aires-da-Silva, A. M., Maunder, M. N., Schaefer, K. M., and Fuller, D. W. 2015. Estimating fish growth for stock assessments using both age-length and tagging-increment data. *Fish. Res.* (2015): <http://dx.doi.org/10.1016/j.fishres.2015.06.011>
- Maunder, M.N., Piner, K.R. 2015. Contemporary fisheries stock assessment: many issues still remain. *ICES Journal of Marine Science* (2015), 72(1), 7–18. doi:10.1093/icesjms/fsu015
- McKechnie, S., Hampton, J., Abascal, F., Davies, N. and Harley, S. J. (2015). Sensitivity of the WCPFC bigeye tuna stock assessment results to the inclusion of EPO dynamics within a Pacific-wide model. [WCPFC-SC11-2015/SA-WP-04](#). Western and Central Pacific Commission. Scientific Committee Eleventh Regular Session. Pohnpei, Federated States of Micronesia, 5-13 August 2015.
- Minte-Vera, C.V., A. Aires-da-Silva, K. Satoh, and M.N. Maunder. 2016. Changes in longline size-frequency data and their effects on the stock assessment models for yellowfin and bigeye tunas. Inter-Amer. Trop. Tuna Comm. 7th Scient. Adv. Com. Meeting SAC-07-04a.
- Satoh, K., C.V. Minte-Vera, N.W. Vogel, A. Aires-da-Silva, C.E. Lennert-Cody, M.N. Maunder, H. Okamoto, K. Uosaki, T. Matsumoto, Y. Semba, T. Ito. 2016. An exploration into Japanese size data of tropical tuna species because of a prominent size-frequency residual pattern in the stock assessment model. Inter-Amer. Trop. Tuna Comm., 7<sup>th</sup> Scient. Adv. Com. Meeting. SAC-07-03d
- Schaefer, K., Fuller, D., Hampton, J., Cailliet, S., Leroy, B., and Itano, D. (2014). Movements, dispersion, and mixing of bigeye tuna (*Thunnus obesus*) tagged and released in the equatorial Central Pacific Ocean, with conventional and archival tags. *Fisheries Research*, 161:336-355.

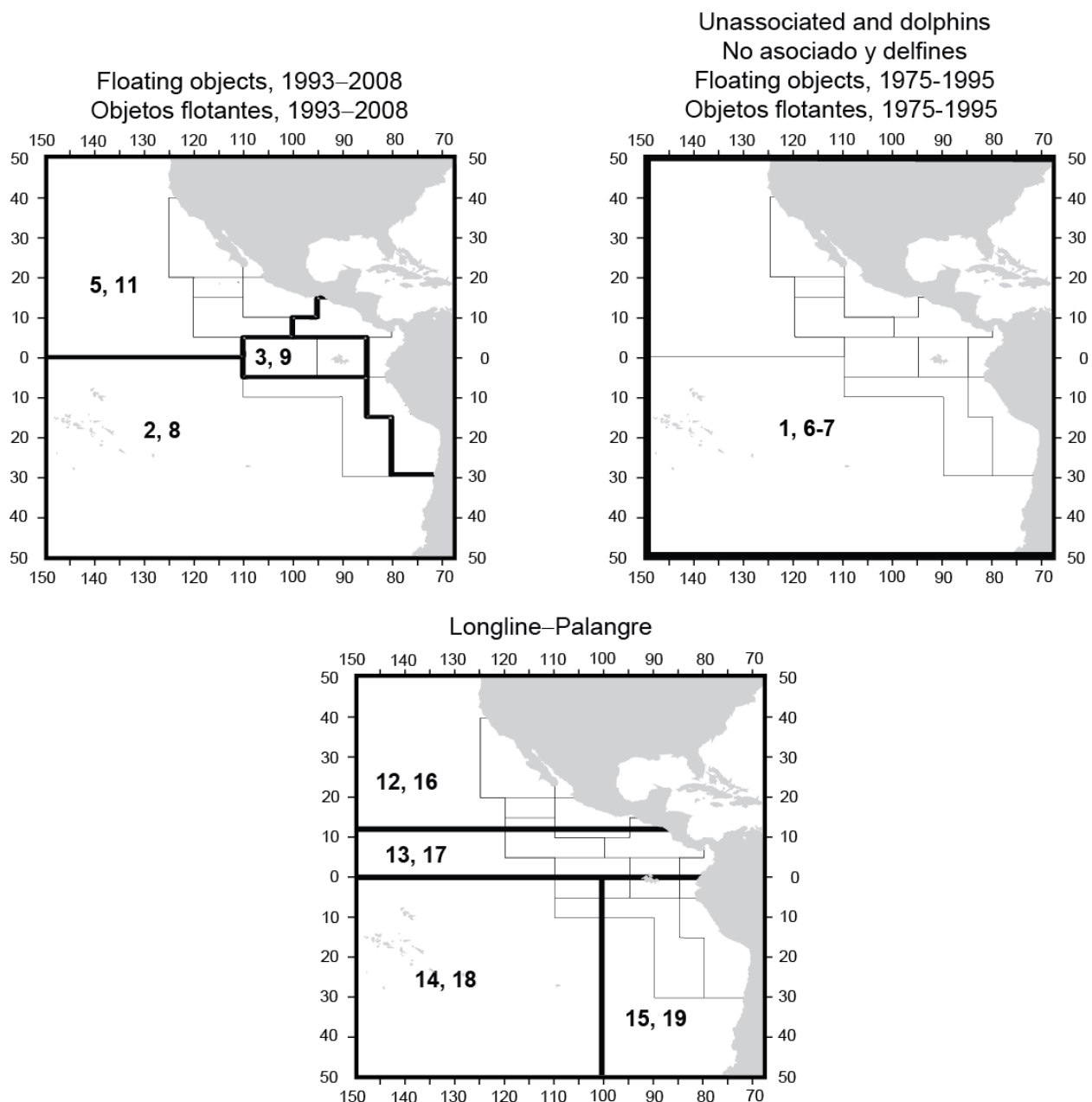


**FIGURE 1.** Spatial extents of the fisheries defined for the stock assessment of bigeye tuna in the EPO. The thin lines indicate the boundaries of 13 length-frequency sampling areas, the bold lines the boundaries of each fishery defined for the stock assessment, and the numbers the fisheries to which the latter boundaries apply. The fisheries are described in Table 1.

**FIGURA 1.** Extensión espacial de las pesquerías definidas para la evaluación de la población de atún patudo en el OPO. Las líneas delgadas indican los límites de 13 zonas de muestreo de frecuencia de tallas, las líneas gruesas los límites de cada pesquería definida para la evaluación de la población, y los números las pesquerías correspondientes a estos últimos límites. En la Tabla 1 se describen las pesquerías.

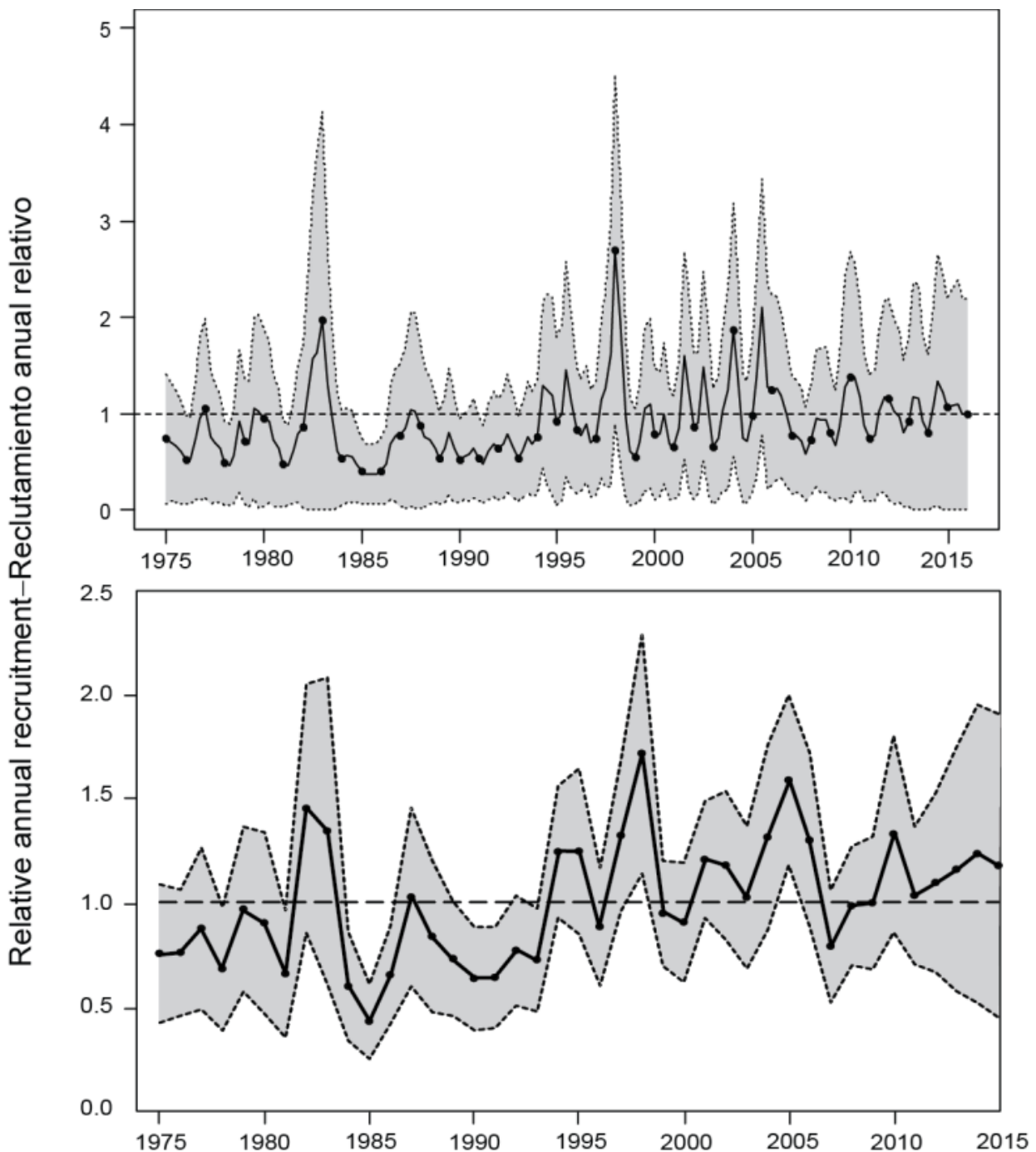


**FIGURE 2.** Estimated quarterly (top panel) and annual (bottom panel) recruitment of bigeye tuna to the fisheries of the EPO. The estimates are scaled so that the estimate of virgin recruitment is equal to 1.0 (dashed horizontal line). The solid line shows the maximum likelihood estimates (MLE) of recruitment, and the shaded area indicates the approximate 95% intervals around those estimates.

**FIGURA 2.** Reclutamiento estimado trimestral (recuadro superior) y anual (recuadro inferior) de atún patudo a las pesquerías del OPO. Se fija la escala de las estimaciones para que la estimación de reclutamiento virgen equivalga a 1,0 (línea de trazos horizontal). La línea sólida indica las estimaciones de verosimilitud máxima (EVM) del reclutamiento, y el área sombreada indica los intervalos de confianza de 95% aproximados de esas estimaciones.

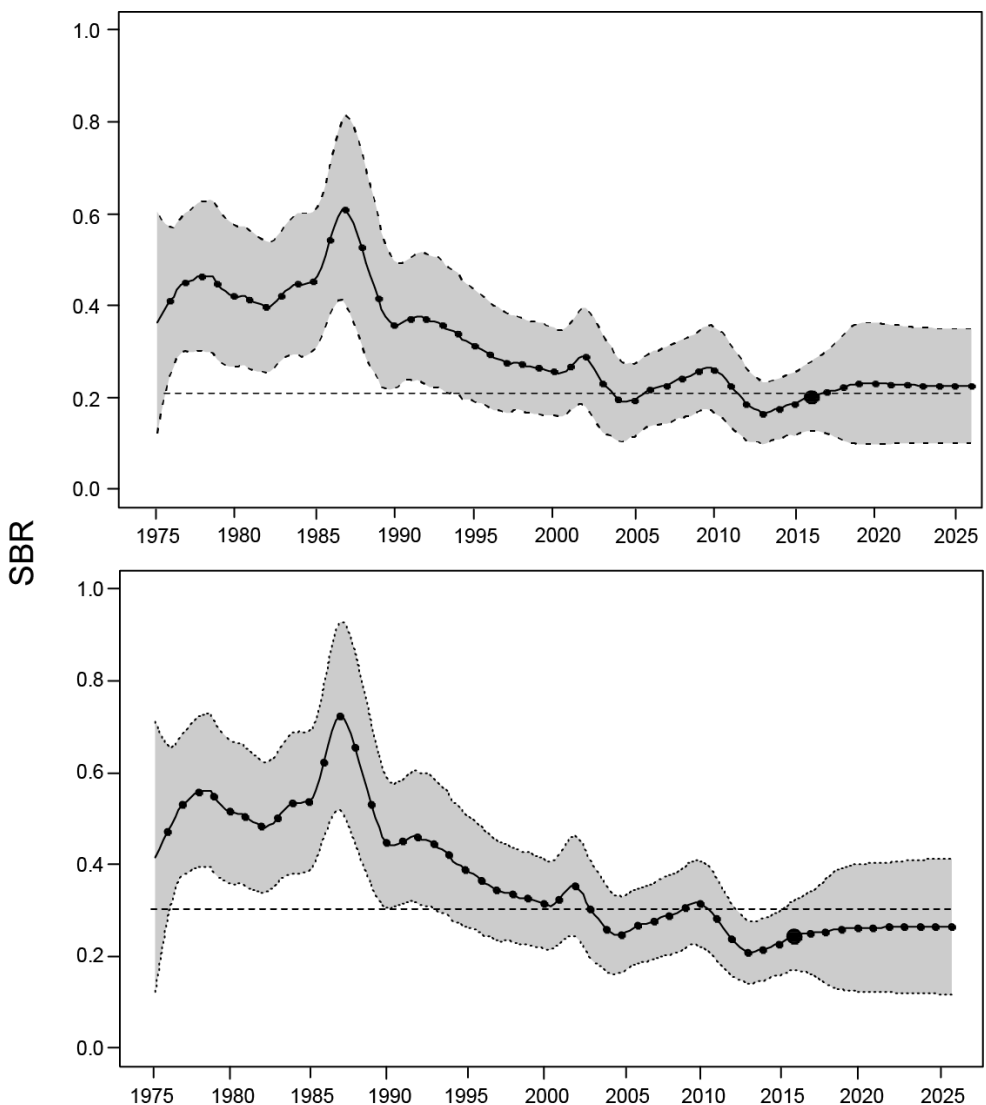


**FIGURE 3.** Estimated spawning biomass ratios (SBRs) of bigeye tuna in the EPO, including projections for 2016-2026 based on average fishing mortality rates during 2013-2015, from the base case (top panel) and the sensitivity analysis that assumes a stock-recruitment relationship ( $h = 0.75$ , bottom panel). The dashed horizontal line (at 0.21 and 0.30, respectively) identifies the SBR at MSY. The solid line illustrates the maximum likelihood estimates, and the estimates after 2016 (the large dot) indicate the SBR predicted to occur if fishing mortality rates continue at the average of that observed during 2013-2015, and recruitment is average during the next 10 years. The shaded area indicates the approximate 95-percent confidence intervals around those estimates.

**FIGURA 3.** Cocientes de biomasa reproductora (SBR) estimados de atún patudo en el OPO, incluyendo proyecciones para 2016-2026 basadas en las tasas medias de mortalidad por pesca durante 2013-2015, del caso base (recuadro superior) y el análisis de sensibilidad que supone una relación población-reclutamiento ( $h = 0.75$ , recuadro inferior). La línea de trazos horizontal (en 0.21 y 0.30, respectivamente) identifica SBR<sub>RMS</sub>. La línea sólida ilustra las estimaciones de verosimilitud máxima, y las estimaciones a partir de 2016 (el punto grande) señalan el SBR que se predice ocurrirá si las tasas de mortalidad por pesca continúan en el promedio observado durante 2013-2015 y el reclutamiento es promedio durante los 10 años próximos. El área sombreada representa los intervalos de confianza de 95% alrededor de esas estimaciones.

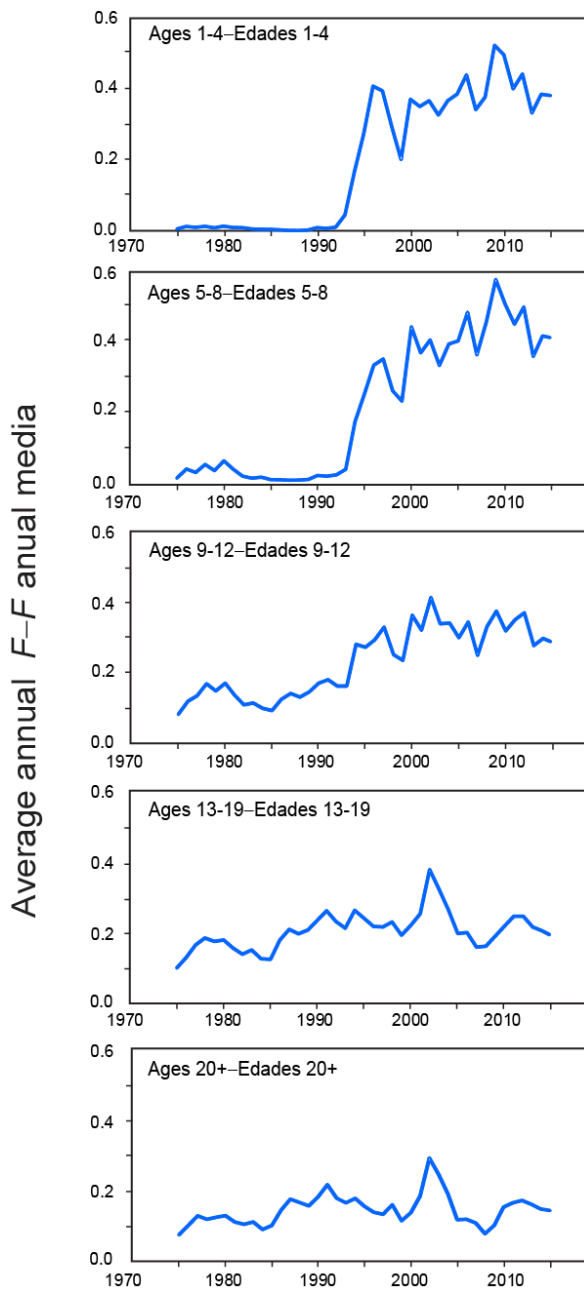


**FIGURE 4.** Average annual fishing mortality, by all gears, of bigeye tuna recruited to the fisheries of the EPO. Each panel illustrates the average fishing mortality rates that affected the fish within the range of ages indicated in the title of each panel. For example, the trend illustrated in the top panel is an average of the fishing mortalities that affected fish that were 1-4 quarters old.

**FIGURA 4.** Mortalidad por pesca anual media, por todas las artes, de atún patudo reclutado a las pesquerías del OPO. Cada recuadro ilustra las tasas medias de mortalidad por pesca que afectaron a los peces de la edad indicada en el título de cada recuadro. Por ejemplo, la tendencia ilustrada en el recuadro superior es un promedio de las mortalidades por pesca que afectaron a los peces de entre 1 y 4 trimestres de edad.

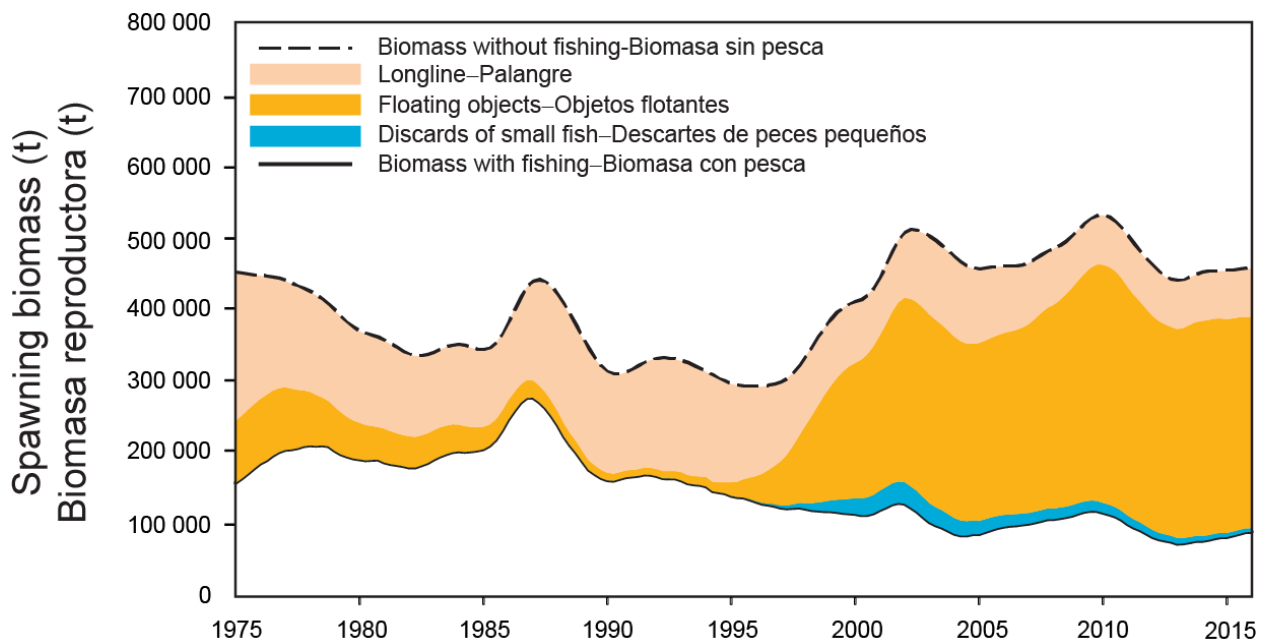


**FIGURE 5.** Trajectory of the spawning biomass of a simulated population of bigeye tuna that was never exploited (top dashed line) and that predicted by the stock assessment model (bottom solid line). The shaded areas between the two lines show the portions of the impact attributed to each fishing method. t = metric tons.

**FIGURA 5.** Trayectoria de la biomasa reproductora de una población simulada de atún patudo nunca explotada (línea de trazos superior) y la que predice el modelo de evaluación (línea sólida inferior). Las áreas sombreadas entre las dos líneas señalan la porción del efecto atribuida a cada método de pesca. t = toneladas.

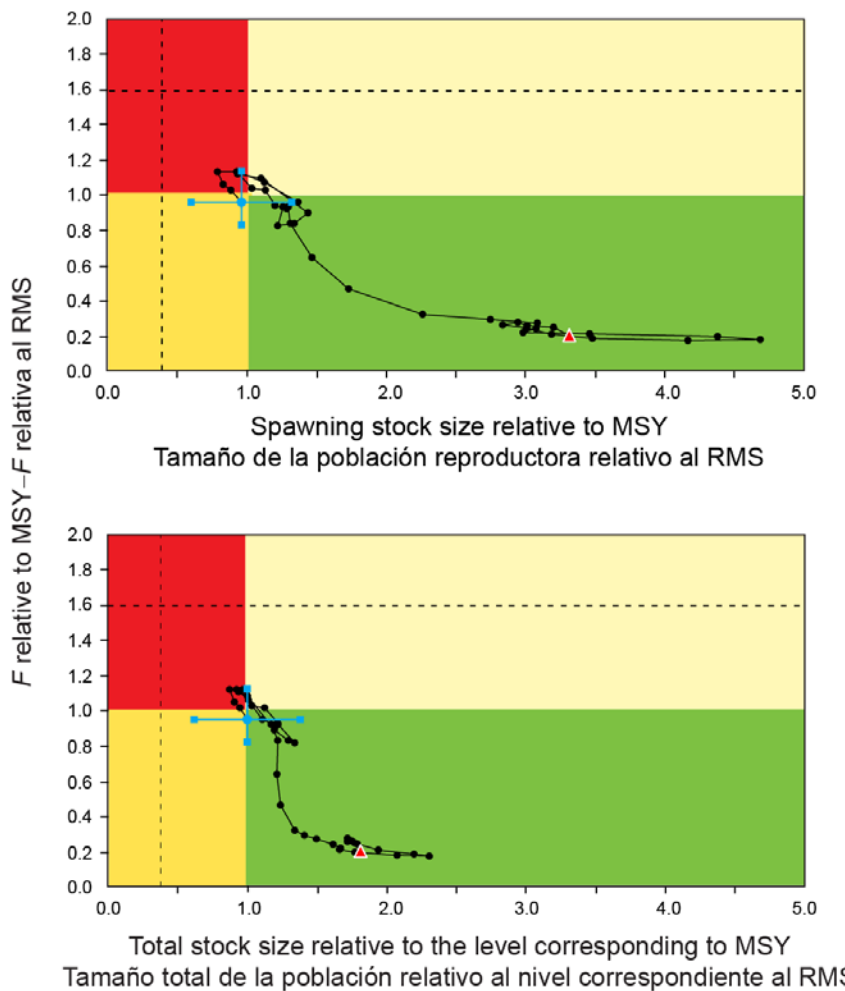


**FIGURE 6.** Kobe (phase) plot of the time series of estimates of spawning stock size (top panel: spawning biomass; bottom panel: total biomass aged 3+ quarters) and fishing mortality relative to their MSY reference points. The colored panels represent interim target reference points ( $S_{MSY}$  and  $F_{MSY}$ ; solid lines) and limit reference points (dashed lines) of  $0.38 S_{MSY}$  and  $1.6 F_{MSY}$ , which correspond to a 50% reduction in recruitment from its average unexploited level based on a conservative steepness value ( $h = 0.75$ ) for the Beverton-Holt stock-recruitment relationship. Each dot is based on the average fishing mortality rate over three years; the large dot indicates the most recent estimate. The squares around the most recent estimate represent its approximate 95% confidence interval. The triangle represents the first estimate (1975).

**FIGURA 6.** Gráfica de Kobe (fase) de la serie de tiempo de las estimaciones del tamaño de la población reproductora (panel superior: biomasa reproductora; panel inferior: biomasa total de edad 3+ trimestres) y la mortalidad por pesca relativas a sus puntos de referencia de RMS. Los recuadros colorados representan los puntos de referencia objetivo provisionales ( $S_{RMS}$  y  $1F_{RMS}$ ; líneas sólidas) y los puntos de referencia límite (líneas de trazo) de  $0,38 S_{RMS}$  y  $1,6 F_{RMS}$ , que corresponden a una reducción de 50% del reclutamiento de su nivel medio no explotado basada en un valor cauteloso ( $h = 0.75$ ) de la inclinación de la relación población-reclutamiento de Beverton-Holt. Cada punto se basa en la tasa de explotación media de un trienio; el punto grande indica la estimación más reciente. Los cuadros alrededor de la estimación más reciente representan su intervalo de confianza de 95% aproximado. El triángulo representa la primera estimación (1975).

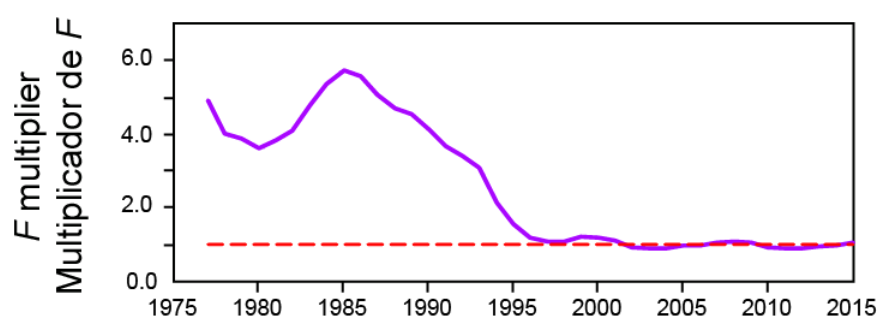
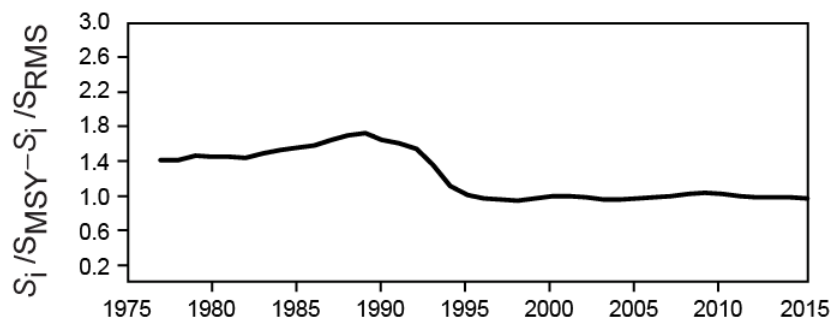
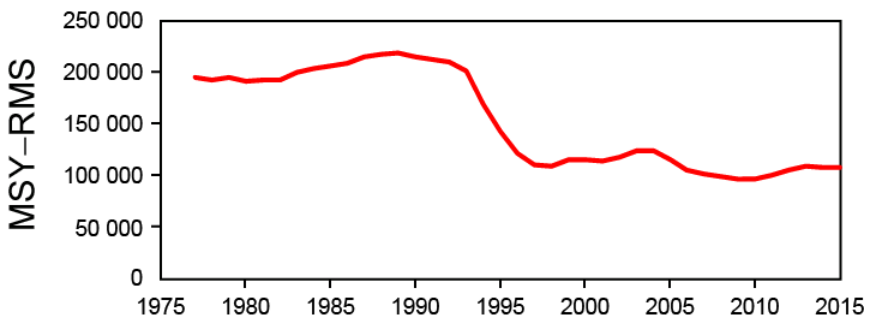
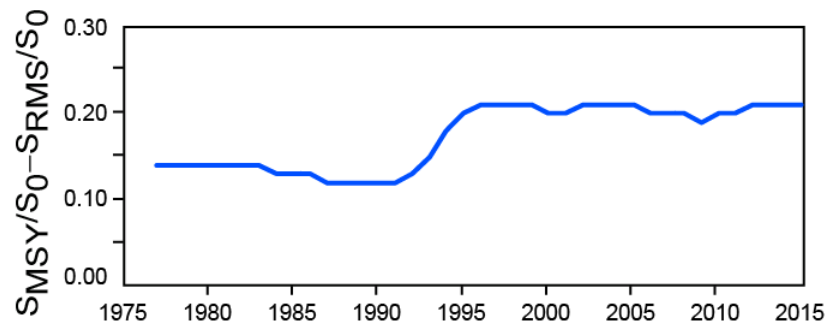


**FIGURE 7.** Estimates of MSY-related quantities calculated using the average age-specific fishing mortality for each year. ( $S_i$  is the spawning biomass at the end of the last year in the assessment.)

**FIGURA 7.** Estimaciones de cantidades relacionadas con el RMS calculadas usando la mortalidad por pesca media por edad de cada año. ( $S_i$  es la biomasa reproductora al fin del último año en la evaluación.)

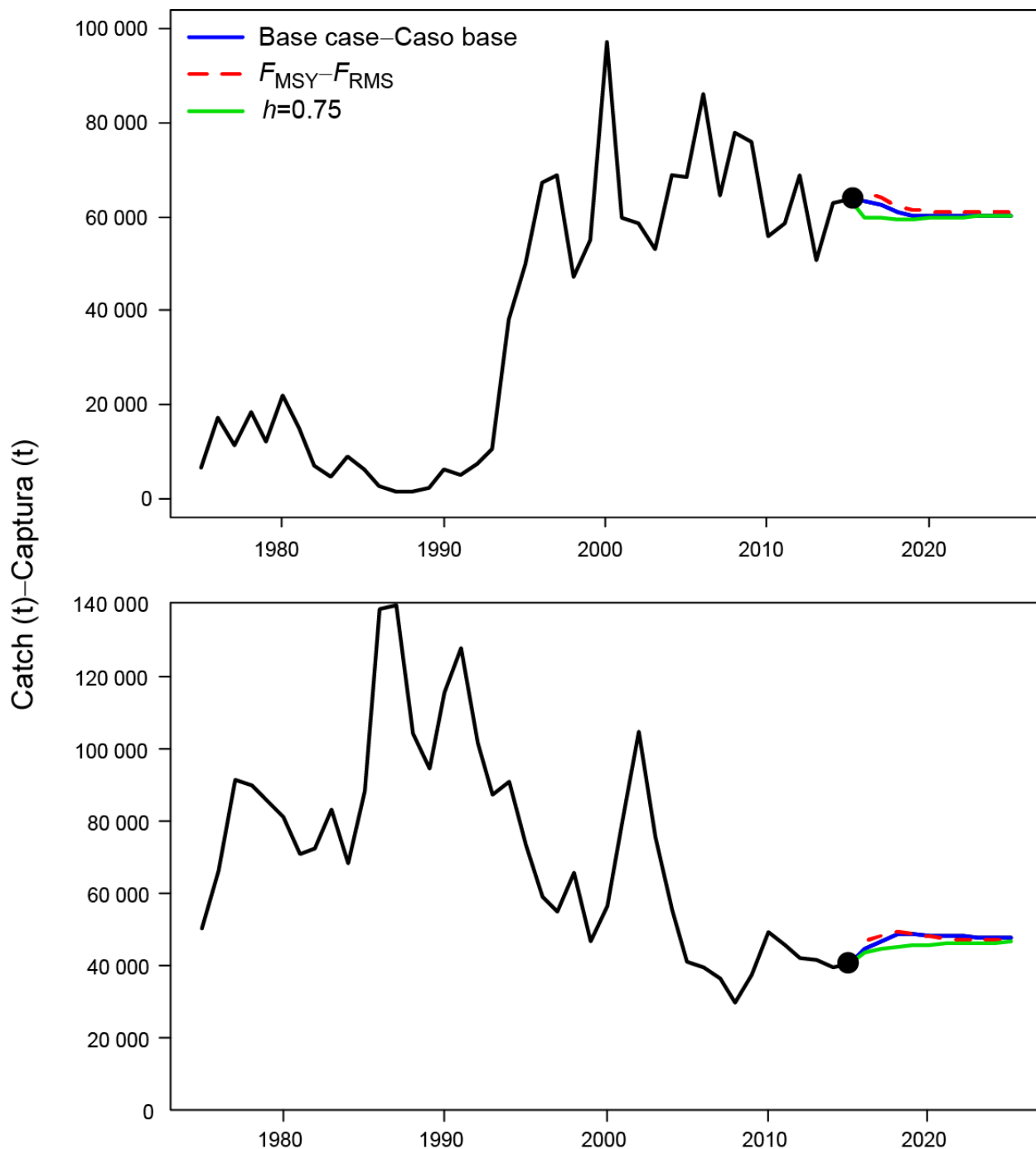


**FIGURE 8.** Historic and projected annual catches of bigeye tuna over a period of 10 years by surface (top panel) and longline (bottom panel), based on fishing mortality rates during 2013-2015. Projected catches are compared between the base case, the analysis assuming  $F_{MSY}$ , and the analysis in which a stock-recruitment relationship ( $h = 0.75$ ) was used. t = metric tons.

**FIGURA 8.** Capturas anuales históricas y proyectadas de atún patudo durante un decenio por las pesquerías de superficie (recuadro superior) y de palangre (recuadro inferior), basadas en las tasas de mortalidad por pesca durante 2013-2015. Se comparan las capturas proyectadas entre el caso base, el análisis que supone  $F_{RMS}$ , y el análisis en el que se usa una relación población-reclutamiento ( $h = 0.75$ ). t = toneladas.

**TABLE 1.** Fisheries defined for the stock assessment of bigeye tuna in the EPO. PS = purse-seine; LP = pole and line; LL = longline; LL-T: longline training vessels; LL-C: commercial longline vessels; OBJ = sets on floating objects; NOA = sets on unassociated fish; DEL = sets on dolphins. The sampling areas are shown in Figure 1.

**TABLA 1.** Pesquerías definidas para la evaluación de la población de atún patudo en el OPO. PS = red de cerco; LP = caña; LL = palangre; LL-T: buques palangreros de aprendizaje; LL-C: buques palangreros comerciales; OBJ = lances sobre objetos flotantes; NOA = lances sobre atunes no asociados; DEL = lances sobre delfines. En la Figura 1 se ilustran las zonas de muestreo.

| Fishery<br>Pesquería | Gear<br>Arte | Set type<br>Tipo lance | Years<br>Años | Sampling areas<br>Zonas de muestreo |  | Catch data<br>Datos de captura   |
|----------------------|--------------|------------------------|---------------|-------------------------------------|--|--|
|                      |              |                        |               | FISHERIES – PESQUERÍAS              |  |  |
| 1                    | PS           | OBJ                    | 1975-1992     | 1-13                                |  | Retained catch only–Captura retenida solamente   |
| 2                    | PS           | OBJ                    | 1993-present  | 11-12                               |  | Retained catch + discards from inefficiencies in fishing process–Captura retenida + descartes de ineficacias en el proceso de pesca            |
| 3                    | PS           | OBJ                    | 1993-present  | 7, 9                                |  |  |
| 4                    | PS           | OBJ                    | 1993-present  | 5-6, 13                             |  |  |
| 5                    | PS           | OBJ                    | 1993-present  | 1-4, 8, 10                          |  |  |
| 6                    | PS<br>LP     | NOA<br>DEL             | 1975-1989     | 1-13                                |  | Retained catch only–Captura retenida solamente   |
| 7                    | PS<br>LP     | NOA<br>DEL             | 1990-present  | 1-13                                |  | Retained catch + discards from inefficiencies in fishing process–Captura retenida + descartes de ineficacias en el proceso de pesca            |
| 8                    | PS           | OBJ                    | 1993-present  | 11-12                               |  | Discards of small fish from size-sorting the catch by Fishery 2 –<br>Descartes de peces pequeños de clasificación por tamaño en la Pesquería 2 |
| 9                    | PS           | OBJ                    | 1993-present  | 7, 9                                |  | Discards of small fish from size-sorting the catch by Fishery 3 –<br>Descartes de peces pequeños de clasificación por tamaño en la Pesquería 3 |
| 10                   | PS           | OBJ                    | 1993-present  | 5-6, 13                             |  | Discards of small fish from size-sorting the catch by Fishery 4 –<br>Descartes de peces pequeños de clasificación por tamaño en la Pesquería 4 |
| 11                   | PS           | OBJ                    | 1993-present  | 1-4, 8, 10                          |  | Discards of small fish from size-sorting the catch by Fishery 5 –<br>Descartes de peces pequeños de clasificación por tamaño en la Pesquería 5 |
| 12                   | LL           | -                      | 1975-present  | N of–de 10°N                        |  | Retained catch only (in numbers)–Captura retenida solamente (en número)  |
| 13                   | LL           | -                      | 1975-present  | N of–de 0° & S of–de 10°N           |  | Retained catch only (in numbers)–Captura retenida solamente (en número)  |
| 14                   | LL           | -                      | 1975-present  | S of–de 0° & W of–de 100°W          |  | Retained catch only (in numbers)–Captura retenida solamente (en número)  |
| 15                   | LL           | -                      | 1975-present  | S of–de 0° & E of–de 100°W          |  | Retained catch only (in numbers)–Captura retenida solamente (en número)  |
| 16                   | LL           | -                      | 1990-present  | N of–de 10°N                        |  | Retained catch only (in weight)–Captura retenida solamente (en peso)   |
| 17                   | LL           | -                      | 1990-present  | N of–de 0° & S of–de 10°N           |  | Retained catch only (in weight)–Captura retenida solamente (en peso)   |
| 18                   | LL           | -                      | 1990-present  | S of–de 0° & W of–de 100°W          |  | Retained catch only (in weight)–Captura retenida solamente (en peso)   |
| 19                   | LL           | -                      | 1990-present  | S of–de 0° & E of–de 100°W          |  | Retained catch only (in weight)–Captura retenida solamente (en peso)   |

**TABLE 1.** (cont.)**TABLA 1.** (continuación)

| Survey<br>Estudio | Gear<br>Arte | Set type<br>Tipo lance | Years<br>Años | Sampling areas<br>Zonas de muestreo |  | Catch data<br>Datos de captura  |
|-------------------|--------------|------------------------|---------------|-------------------------------------|--|---|
|                   |              |                        |               | SURVEYS – ESTUDIOS                  |  |   |
| 1                 | LL-T         | -                      | 1975-present  | N of–de 10°N                        |  | No catches, length-composition data- Sin capturas, datos de composición por talla   |
| 2                 | LL-T         | -                      | 1975-present  | N of–de 0° & S of–de 10°N           |  | No catches, length-composition data- Sin capturas, datos de composición por talla   |
| 3                 | LL-T         | -                      | 1975-present  | S of–de 0° & W of–de 100°W          |  | No catches, length-composition data- Sin capturas, datos de composición por talla   |
| 4                 | LL-T         | -                      | 1975-present  | S of–de 0° & E of–de 100°W          |  | No catches, length-composition data- Sin capturas, datos de composición por talla   |
| 5                 | LL-C         | -                      | 1975-1994     | N of–de 10°N                        |  | No catches, weight-composition data (not used to fit the model)<br>Sin capturas, datos de composición por peso (no usados para ajustar el modelo) |
| 6                 | LL-C         | -                      | 1975-1994     | N of–de 0° & S of–de 10°N           |  | No catches, weight-composition data (not used to fit the model)<br>Sin capturas, datos de composición por peso (no usados para ajustar el modelo) |
| 7                 | LL-C         | -                      | 1975-1994     | S of–de 0° & W of–de 100°W          |  | No catches, weight-composition data (not used to fit the model)<br>Sin capturas, datos de composición por peso (no usados para ajustar el modelo) |
| 8                 | LL-C         | -                      | 1975-1994     | S of–de 0° & E of–de 100°W          |  | No catches, weight-composition data (not used to fit the model)<br>Sin capturas, datos de composición por peso (no usados para ajustar el modelo) |

**TABLE 2.** Estimates of the MSY and its associated quantities for bigeye tuna for the base case assessment and the sensitivity analyses. All analyses are based on average fishing mortality during 2013-2015.  $B_{\text{recent}}$  and  $B_{\text{MSY}}$  are defined as the biomass of fish 3+ quarters old (in metric tons) at the beginning of 2016 and at MSY, respectively.  $S_{\text{recent}}$  and  $S_{\text{MSY}}$  are in metric tons.  $C_{\text{recent}}$  is the estimated total catch in 2015. The  $F$  multiplier indicates how many times effort would have to be effectively increased to achieve the MSY in relation to the average fishing mortality during 2013-2015.

**TABLA 2.** Estimaciones del RMS y sus cantidades asociadas para el atún patudo para la evaluación del caso base y los análisis de sensibilidad. Todos los análisis se basan en la mortalidad por pesca promedio de 2013-2015. Se definen  $B_{\text{recent}}$  y  $B_{\text{RMS}}$  como la biomasa de peces de 3+ trimestres de edad (en toneladas) al principio de 2016 y en RMS, respectivamente. Se expresan  $S_{\text{recent}}$  y  $S_{\text{MSY}}$  en toneladas métricas.  $C_{\text{recent}}$  es la captura total estimada en 2015. El multiplicador de  $F$  indica cuántas veces se tendría que incrementar el esfuerzo para lograr el RMS en relación con la mortalidad por pesca media durante 2013-2015.

|   | Base case-<br>Caso base | $h = 0.75$ |
|---|-------------------------|------------|
| MSY-RMS   | 107,864                 | 107,595    |
| $B_{\text{MSY}} - B_{\text{RMS}}$                                     | 389,211                 | 726,606    |
| $S_{\text{MSY}} - S_{\text{RMS}}$                                     | 95,101                  | 200,215    |
| $B_{\text{MSY}}/B_0 - B_{\text{RMS}}/B_0$                             | 0.26                    | 0.34       |
| $S_{\text{MSY}}/S_0 - S_{\text{RMS}}/S_0$                             | 0.21                    | 0.30       |
| $C_{\text{recent}}/\text{MSY} - C_{\text{recent}}/\text{RMS}$         | 0.97                    | 0.97       |
| $B_{\text{recent}}/B_{\text{MSY}} - B_{\text{recent}}/B_{\text{RMS}}$ | 1.00                    | 0.83       |
| $S_{\text{recent}}/S_{\text{MSY}} - S_{\text{recent}}/S_{\text{RMS}}$ | 0.96                    | 0.81       |
| $F$ multiplier-<br>Multiplicador de $F$                               | 1.05                    | 0.91       |

## APPENDICES - ANEXOS

### APPENDIX A: MODEL DIAGNOSTICS ANEXO A: DIAGNÓSTICOS DEL MODELO

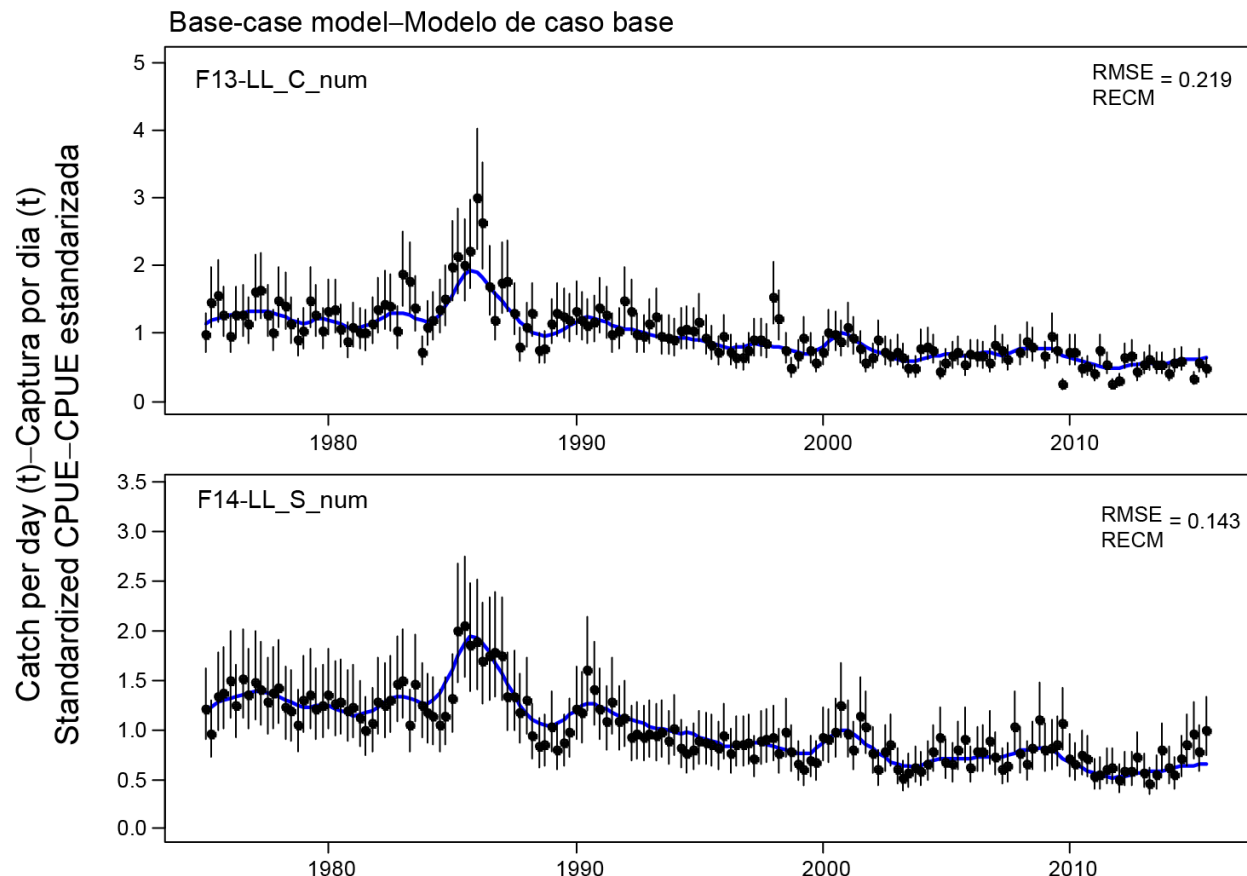


**FIGURE A.1a.** Base case model fit (blue line) to the CPUE of the Central (F13-LL\_C) and Southern (F14-LL\_S) longline fisheries (Table 1). The vertical lines represent the fixed confidence intervals ( $\pm 2$  standard deviations) around the CPUE values. RMSE is the root mean square error of the model fit to the CPUE.

**FIGURA A.1a.** Ajuste del modelo de caso base (línea azul) a la CPUE de las pesquerías palangreras central (F13-LL\_C) y del sur (F14-LL\_S) (Tabla 1). Las líneas verticales representan los intervalos de confianza fijos ( $\pm 2$  desviaciones estándar) alrededor de los valores de CPUE. RECM es la raíz del error cuadrado medio del ajuste del modelo a la CPUE.

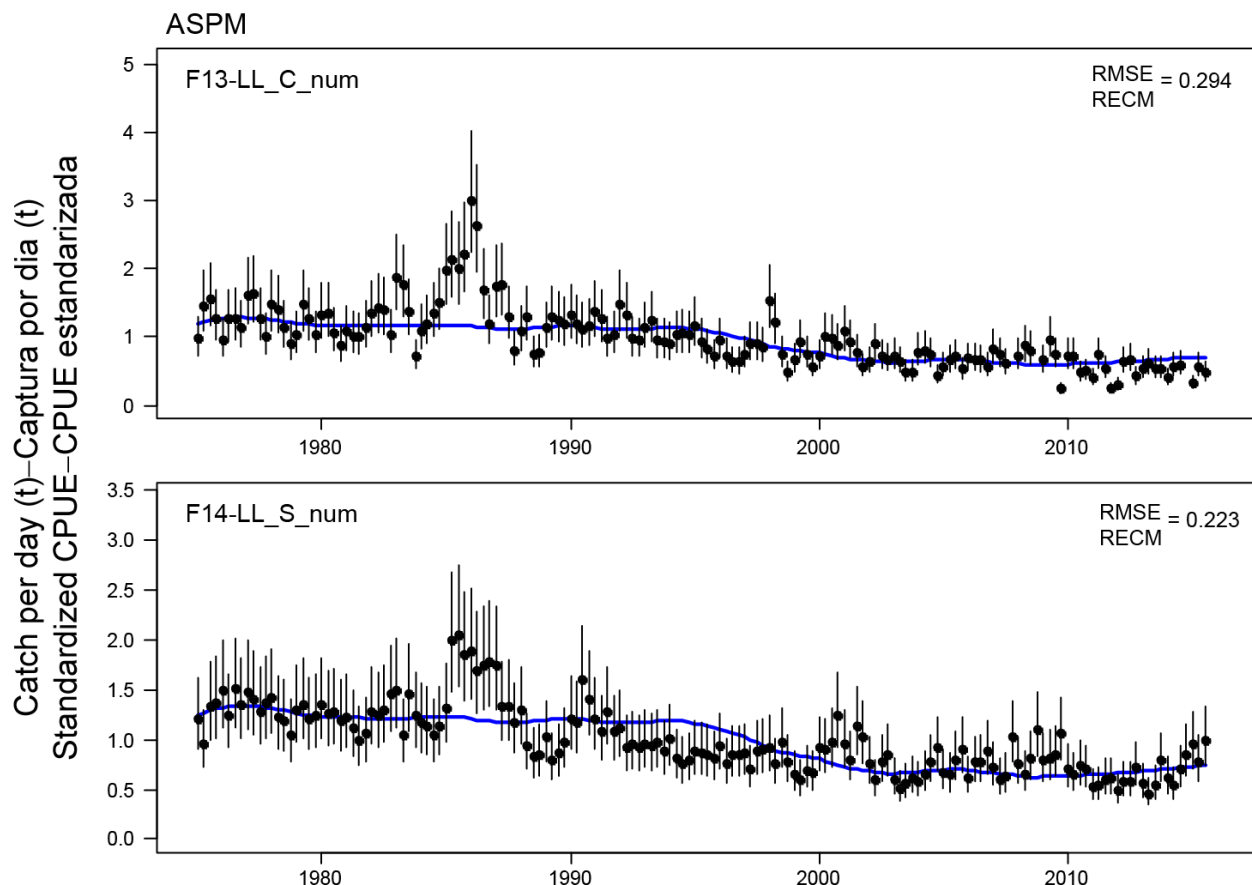


**FIGURE A.1b.** Age-structured production model (ASPM) diagnostic, with no recruitment deviates estimated. Model fit (blue line) to the CPUE of the Central (F13-LL\_C) and Southern (F14-LL\_S) longline fisheries (Table 1). The vertical lines represent the fixed confidence intervals ( $\pm 2$  standard deviations) around the CPUE values. RMSE is the root mean square error of the model fit to the CPUE.

**FIGURA A.1b.** Diagnóstico de modelo de producción por edad (ASPM), sin desviaciones del reclutamiento estimadas. Ajuste del modelo (línea azul) a la CPUE de las pesquerías palangreras central (F13-LL\_C) y del sur (F14-LL\_S) (Tabla 1). Las líneas verticales representan los intervalos de confianza fijos ( $\pm 2$  desviaciones estándar) alrededor de los valores de CPUE. RECM es la raíz del error cuadrado medio del ajuste del modelo a la CPUE.

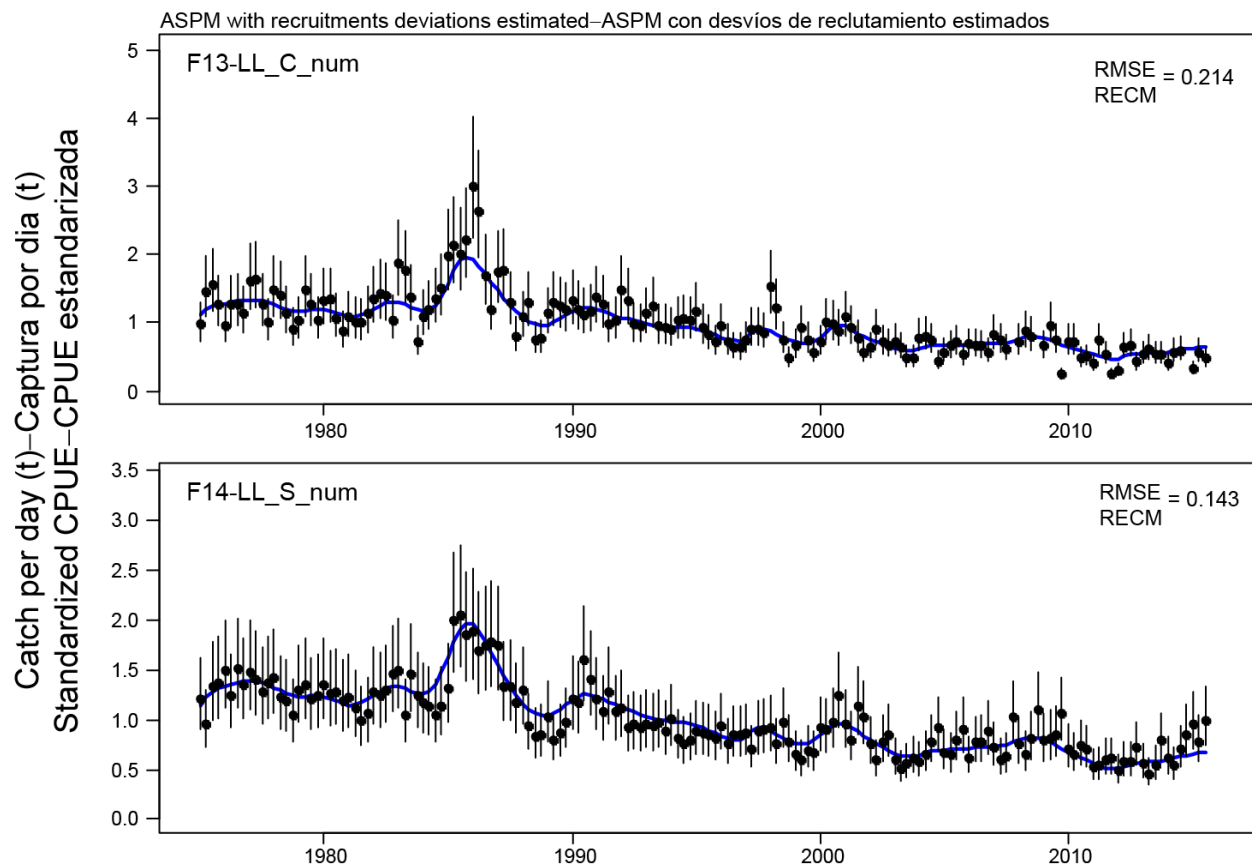


**FIGURE A.1c.** Age-structured production model (ASPM) diagnostic, with recruitment deviates estimated. Model fit (blue line) to the CPUE of the Central (F13-LL\_C) and Southern (F14-LL\_S) longline fisheries (Table 1). The vertical lines represent the fixed confidence intervals ( $\pm 2$  standard deviations) around the CPUE values. RMSE is the root mean square error of the model fit to the CPUE.

**FIGURA A.1c.** Diagnóstico de modelo de producción por edad (ASPM), con desviaciones del reclutamiento estimadas. Ajuste del modelo (línea azul) a la CPUE de las pesquerías palangreras central (F13-LL\_C) y del sur (F14-LL\_S) (Tabla 1). Las líneas verticales representan los intervalos de confianza fijos ( $\pm 2$  desviaciones estándar) alrededor de los valores de CPUE. RECM es la raíz del error cuadrado medio del ajuste del modelo a la CPUE. RECM es la raíz del error cuadrado medio del ajuste del modelo a la CPUE.

ASPM with recruitment deviations set to the base-case model estimates  
 ASPM con desvíos de reclutamiento fijos a los valores estimados por el modelo de caso base

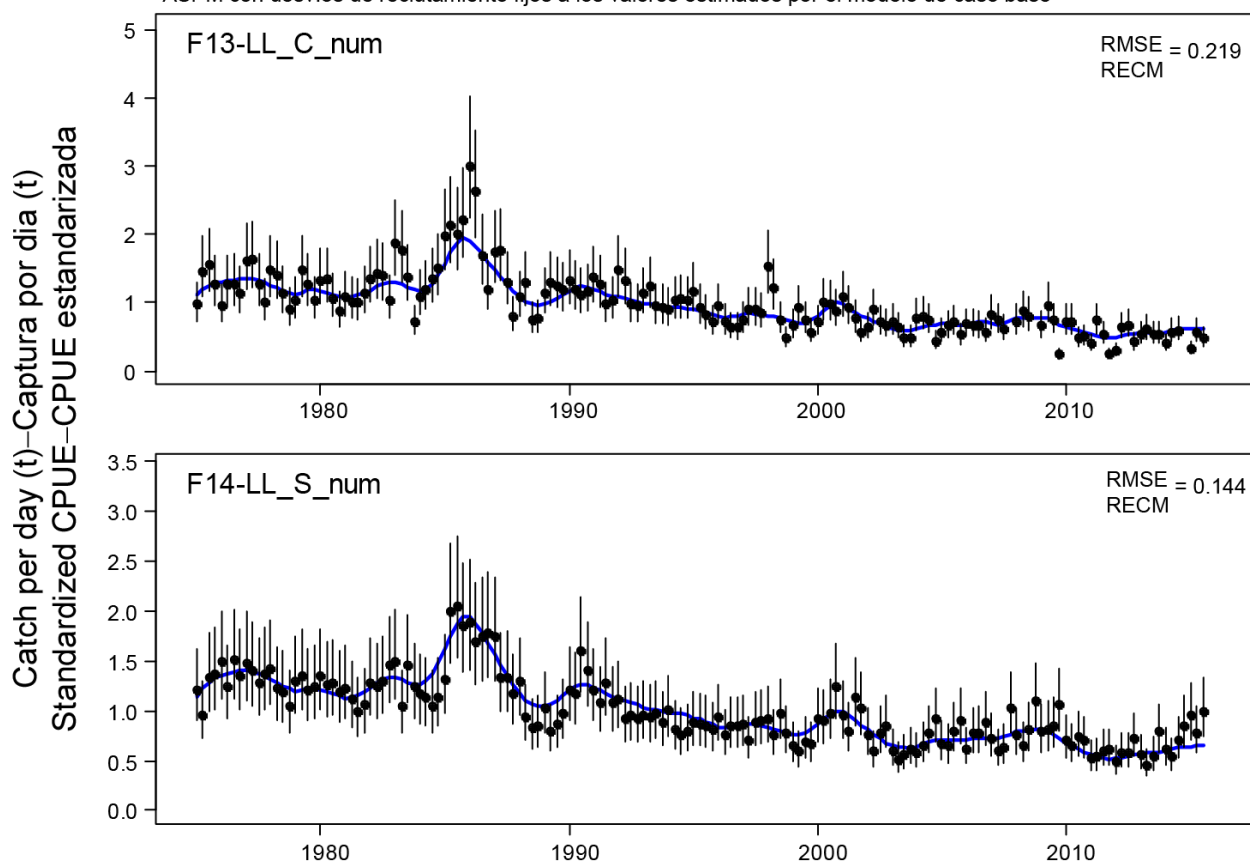


**FIGURE A.1d.** Age-structured production model (ASPM) diagnostic, with recruitment deviates fixed at the estimates of the base case model. Model fit (blue line) to the CPUE of the Central (F13-LL\_C) and Southern (F14-LL\_S) longline fisheries (Table 1). The vertical lines represent the fixed confidence intervals ( $\pm 2$  standard deviations) around the CPUE values. RMSE is the root mean square error of the model fit to the CPUE.

**FIGURA A.1d.** Diagnóstico de modelo de producción por edad (ASPM), con desviaciones del reclutamiento fijadas en las estimaciones del modelo de caso base. Ajuste del modelo (línea azul) a la CPUE de las pesquerías palangreras central (F13-LL\_C) y del sur (F14-LL\_S) (Tabla 1). Las líneas verticales representan los intervalos de confianza fijos ( $\pm 2$  desviaciones estándar) alrededor de los valores de CPUE. RECM es la raíz del error cuadrado medio del ajuste del modelo a la CPUE.

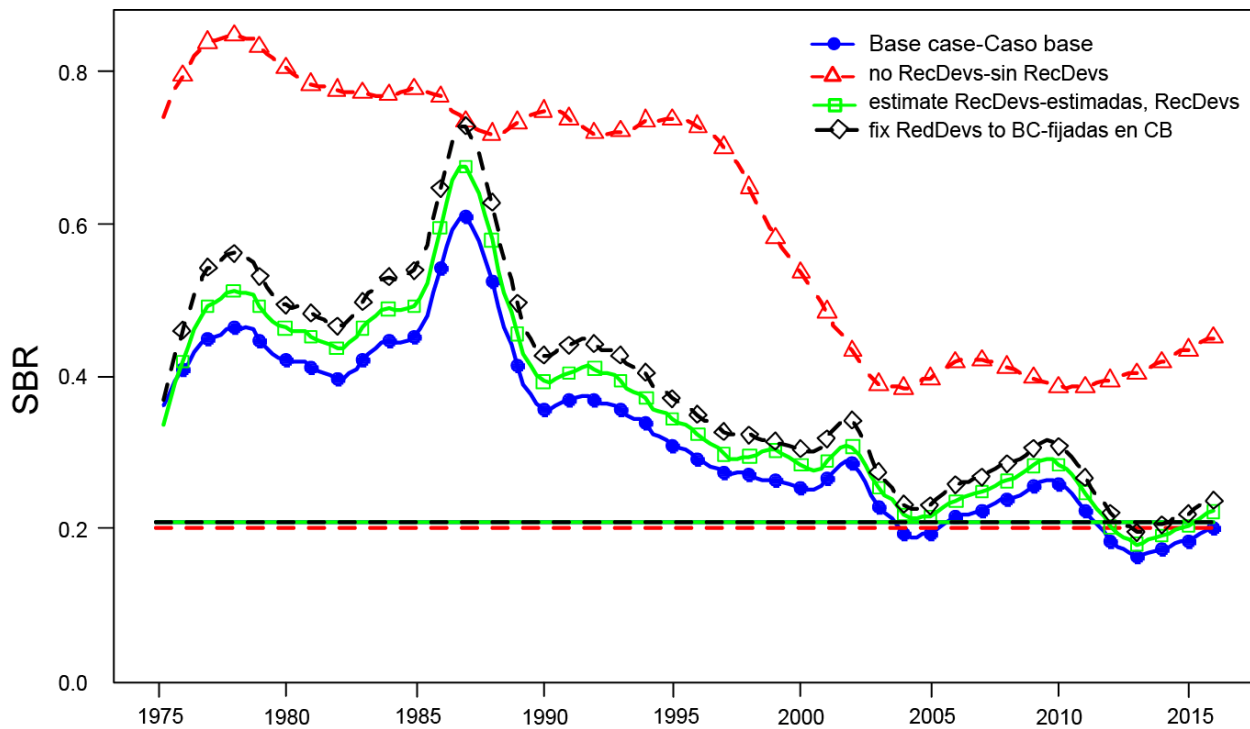


**FIGURE A.2.** Comparison of estimates of the spawning biomass ratio (SBR) of bigeye tuna from the age-structured production model (ASPM) diagnostic. SBR trends are shown for the base case, ASPM with no recruitment deviations estimated, ASPM with recruitment deviations estimated, and ASPM with recruitment deviations fixed at the estimates from the base case model. The horizontal lines represent the SBRs associated with MSY for each scenario.

**FIGURA A.2.** Comparación de las estimaciones del cociente de biomasa reproductora (SBR) de patudo del diagnóstico del modelo de producción por edad (ASPM). Se ilustran las tendencias del SBR correspondientes al caso base, ASPM sin desviaciones del reclutamiento estimadas, ASPM con desviaciones del reclutamiento estimadas, y ASPM con las desviaciones del reclutamiento fijadas en las estimaciones del modelo de caso base. Las líneas horizontales representan los SBR asociados al RMS en cada escenario.

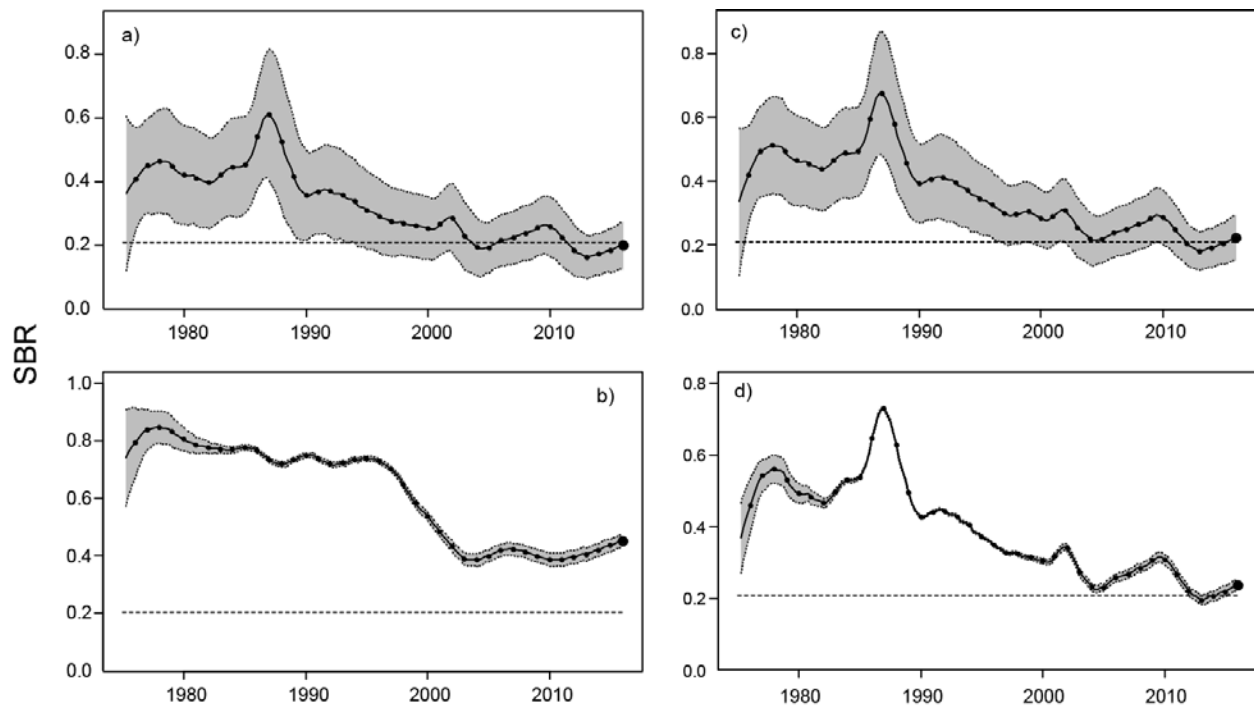


**FIGURE A.3.** Comparison of estimates of the spawning biomass ratio (SBR) of bigeye tuna from the age-structured production model (ASPM) diagnostic. SBR trends are shown for: a) base case, b) ASPM with no recruitment deviations estimated, c) ASPM with recruitment deviations estimated, and d) ASPM with recruitment deviations fixed at the estimates from the base case model. The solid line illustrates the maximum likelihood estimates. The shaded area indicates the approximate 95-percent confidence intervals around those estimates. The horizontal lines represent the SBRs associated with MSY for each scenario.

**FIGURA A.3.** Comparación de las estimaciones del cociente de biomasa reproductora (SBR) de atún patudo del diagnóstico del modelo de producción por edad (ASPM). Se señalan las tendencias del SBR correspondientes al a) caso base, b) ASPM sin desvíos del reclutamiento estimados, c) ASPM con desvíos del reclutamiento estimados, y d) ASPM con los desvíos del reclutamiento fijos en las estimaciones del modelo de caso base. El área sombreada indica los intervalos de confianza de 95% aproximados alrededor de esas estimaciones. Las líneas horizontales representan los SBR asociados al RMS para cada escenario.

**APPENDIX B: SENSITIVITY ANALYSIS FOR STEEPNESS**  
**ANEXO B: ANÁLISIS DE SENSIBILIDAD A LA INCLINACIÓN**

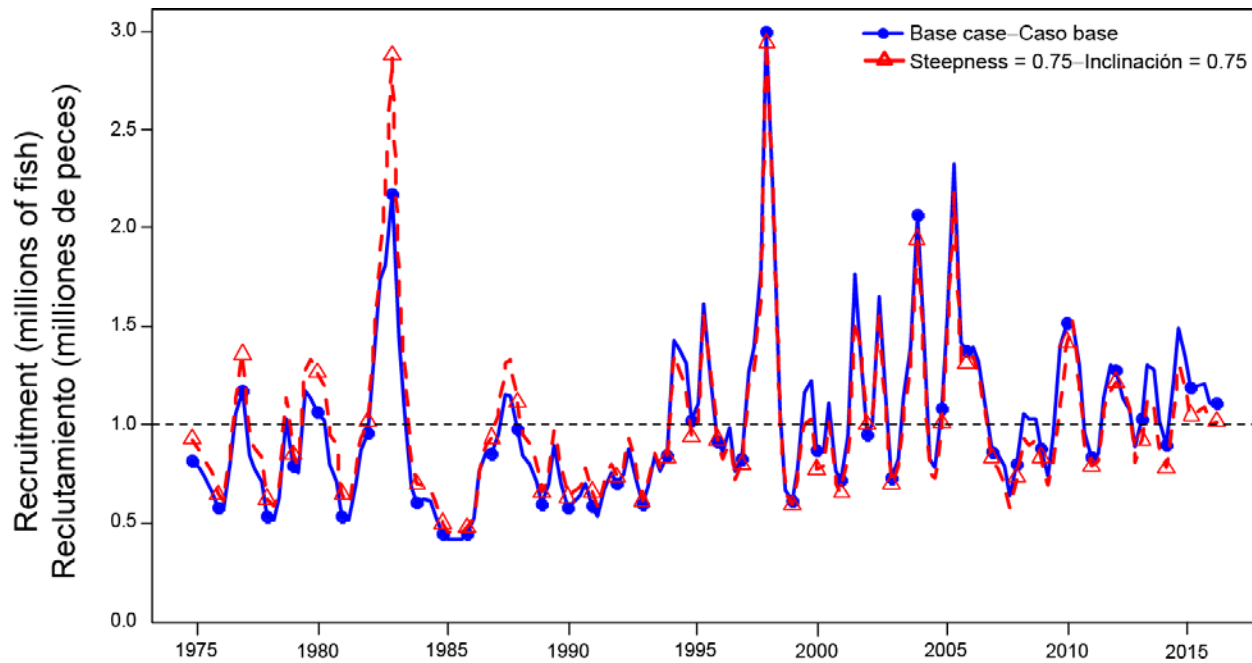


**FIGURE B.1.** Comparison of estimates of relative recruitment for bigeye tuna from the analysis without a stock-recruitment relationship (base case) and with a stock-recruitment relationship (steepness = 0.75). The estimates are scaled so that the estimate of average recruitment is equal to 1.0 (dashed horizontal line).

**FIGURA B.1.** Comparación de las estimaciones de reclutamiento relativo de atún patudo del análisis con (inclinación = 0.75) y sin (caso base) una relación población-reclutamiento. Se fija la escala de las estimaciones para que la estimación de reclutamiento medio equivalga a 1,0 (línea de trazos horizontal).

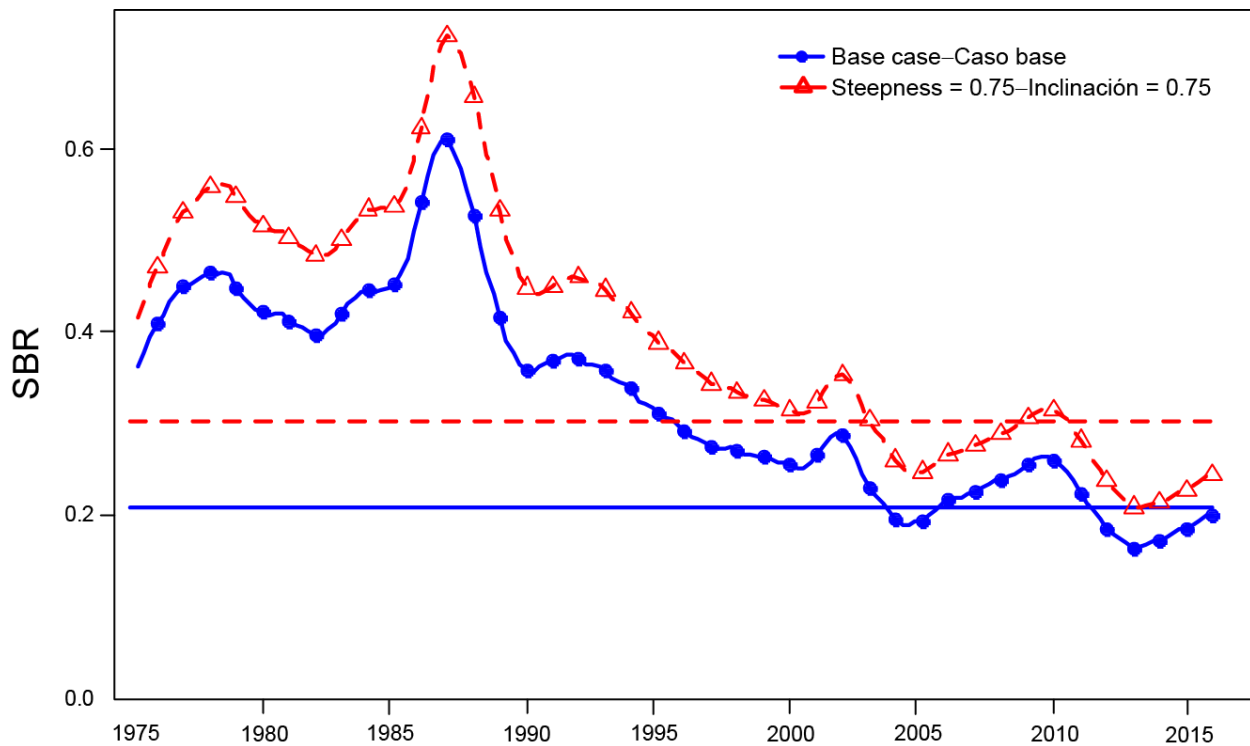


**FIGURE B.2.** Comparison of estimates of the spawning biomass ratio (SBR) of bigeye tuna from the analysis without a stock-recruitment relationship (base case) and with a stock-recruitment relationship (steepness = 0.75). The horizontal lines represent the SBRs associated with MSY in each scenario.

**FIGURA B.2.** Comparación de las estimaciones del cociente de biomasa reproductora (SBR) de atún patudo del análisis con (inclinación = 0.75) y sin (caso base) una relación población-reclutamiento. Las líneas horizontales representan los SBR asociados al RMS en cada escenario.

**TABLE B.1.** Estimates of the MSY and its associated quantities for bigeye tuna for different assumptions on steepness ( $h$ ). All analyses are based on average fishing mortality during 2013-2015.  $B_{\text{recent}}$  and  $B_{\text{MSY}}$  are defined as the biomass of fish 3+ quarters old (in metric tons) at the beginning of 2016 and at MSY, respectively.  $S_{\text{recent}}$  and  $S_{\text{MSY}}$  are in metric tons.  $C_{\text{recent}}$  is the estimated total catch in 2015. The  $F$  multiplier indicates how many times effort would have to be effectively increased to achieve the MSY in relation to the average fishing mortality during 2013-2015.

**TABLA B.1.** Estimaciones del RMS y sus cantidades asociadas para el atún patudo correspondientes a distintos supuestos de la inclinación ( $h$ ). Todos los análisis se basan en la mortalidad por pesca promedio de 2013-2015. Se definen  $B_{\text{recent}}$  y  $B_{\text{RMS}}$  como la biomasa de peces de 3+ trimestres de edad (en toneladas) al principio de 2016 y en RMS, respectivamente. Se expresan  $S_{\text{recent}}$  y  $S_{\text{MSY}}$  en toneladas.  $C_{\text{recent}}$  es la captura total estimada en 2015. El multiplicador de  $F$  indica cuántas veces se tendría que incrementar el esfuerzo para lograr el RMS en relación con la mortalidad por pesca media durante 2013-2015.

|   | Base case-<br>Caso base | $h = 0.75$ |
|---|-------------------------|------------|
| MSY-RMS   | 107,864                 | 107,595    |
| $B_{\text{MSY}} - B_{\text{RMS}}$                                     | 389,211                 | 726,606    |
| $S_{\text{MSY}} - S_{\text{RMS}}$                                     | 95,101                  | 200,215    |
| $B_{\text{MSY}}/B_0 - B_{\text{RMS}}/B_0$                             | 0.26                    | 0.34       |
| $S_{\text{MSY}}/S_0 - S_{\text{RMS}}/S_0$                             | 0.21                    | 0.30       |
| $C_{\text{recent}}/\text{MSY} - C_{\text{recent}}/\text{RMS}$         | 0.97                    | 0.97       |
| $B_{\text{recent}}/B_{\text{MSY}} - B_{\text{recent}}/B_{\text{RMS}}$ | 1.00                    | 0.83       |
| $S_{\text{recent}}/S_{\text{MSY}} - S_{\text{recent}}/S_{\text{RMS}}$ | 0.96                    | 0.81       |
| $F$ multiplier-Multiplicador de $F$                                   | 1.05                    | 0.91       |

**APPENDIX C: SENSITIVITY ANALYSIS TO THE WEIGHTING ASSIGNED TO THE SIZE-COMPOSITION DATA**  
**ANEXO C: ANÁLISIS DE SENSIBILIDAD A LA PONDERACIÓN ASIGNADA A LOS DATOS DE COMPOSICIÓN**  
**POR TALLA**

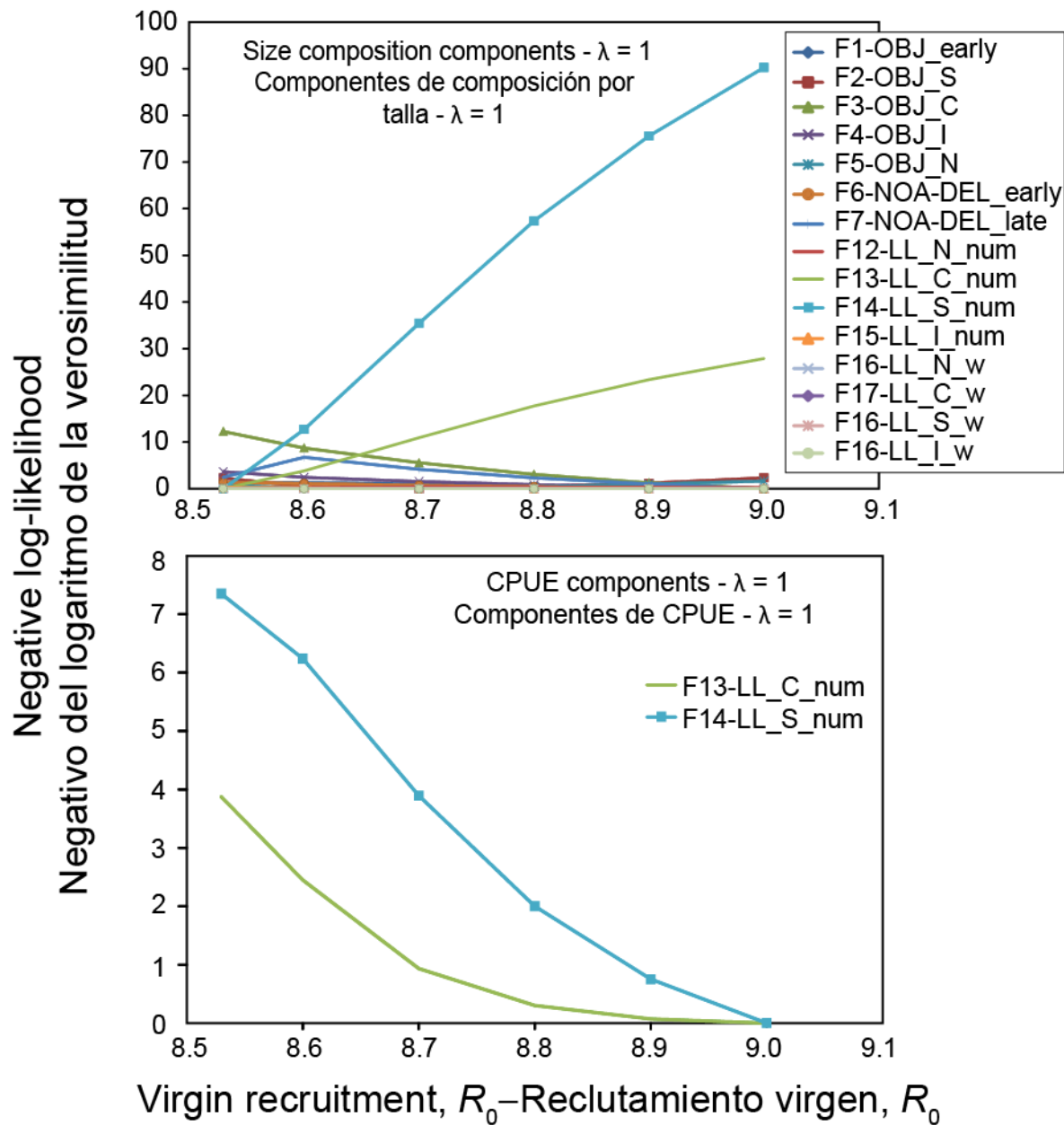


**FIGURE C.1.** Likelihood profile for the virgin recruitment ( $R_0$ ) parameter estimated for a model assuming the base case model configuration, except that the original ( $\lambda = 1$ ), rather than down-weighted ( $\lambda = 0.05$ ), input sample sizes of the size composition data are used. Each line represents the profile for each data component included in the model fit.

**FIGURA C.1.** Perfil de verosimilitud del parámetro de reclutamiento virgen ( $R_0$ ) estimado para un modelo que supone la configuración de caso case, excepto que se usa el tamaño de las muestras originales ( $\lambda = 1$ ) de los datos de composición por talla, no con ponderación reducida ( $\lambda = 0.05$ ). Cada línea representa el perfil de cada componente de datos incluido en el ajuste del modelo.

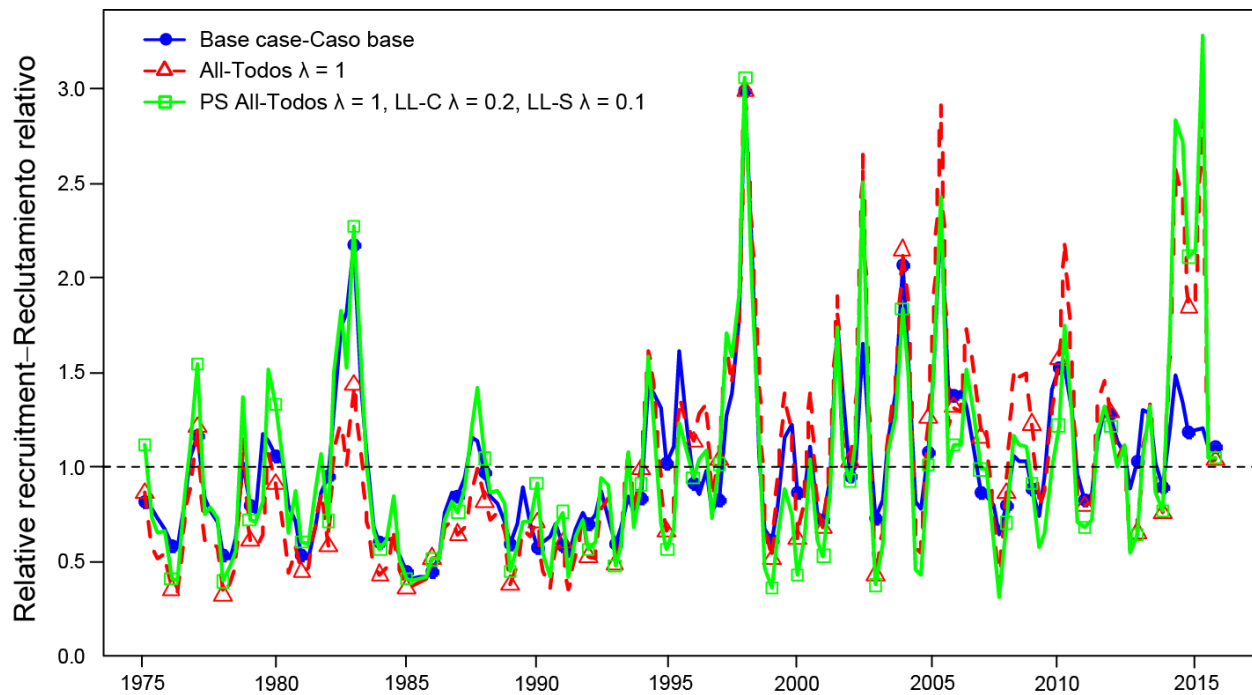


**FIGURE C.2.** Comparison of estimates of relative recruitment of bigeye tuna from the base case analysis (blue dots;  $\lambda = 0.05$  for all fisheries) and two sensitivity analyses: 1) using the original input sample sizes of the size composition data of all fisheries ( $\lambda = 1$ , red triangles); 2) same as 1, except the logistic longline fisheries, whose size composition data are down-weighted (Fisheries 13-14;  $\lambda = 0.2$  and 0.1, respectively, green squares). The estimates are scaled so that the estimate of average recruitment is equal to 1.0 (dashed horizontal line).

**FIGURA C.2.** Comparación de estimaciones del reclutamiento relativo de atún patudo del análisis de caso base (puntos azules;  $\lambda = 0.05$  para todas las pesquerías) y dos análisis de sensibilidad: 1) usar el tamaño de muestra original de los datos de composición por talla de todas las pesquerías ( $\lambda = 1$ , triángulos rojos); 2) igual que 1, excepto las pesquerías palangreras logísticas con datos de composición por talla de ponderación reducida (Pesquerías 13-14;  $\lambda = 0.2$  y 0.1, respectivamente, cuadrados verdes). Se fija la escala de las estimaciones para que la estimación de reclutamiento medio equivalga a 1,0 (línea de trazos horizontal).

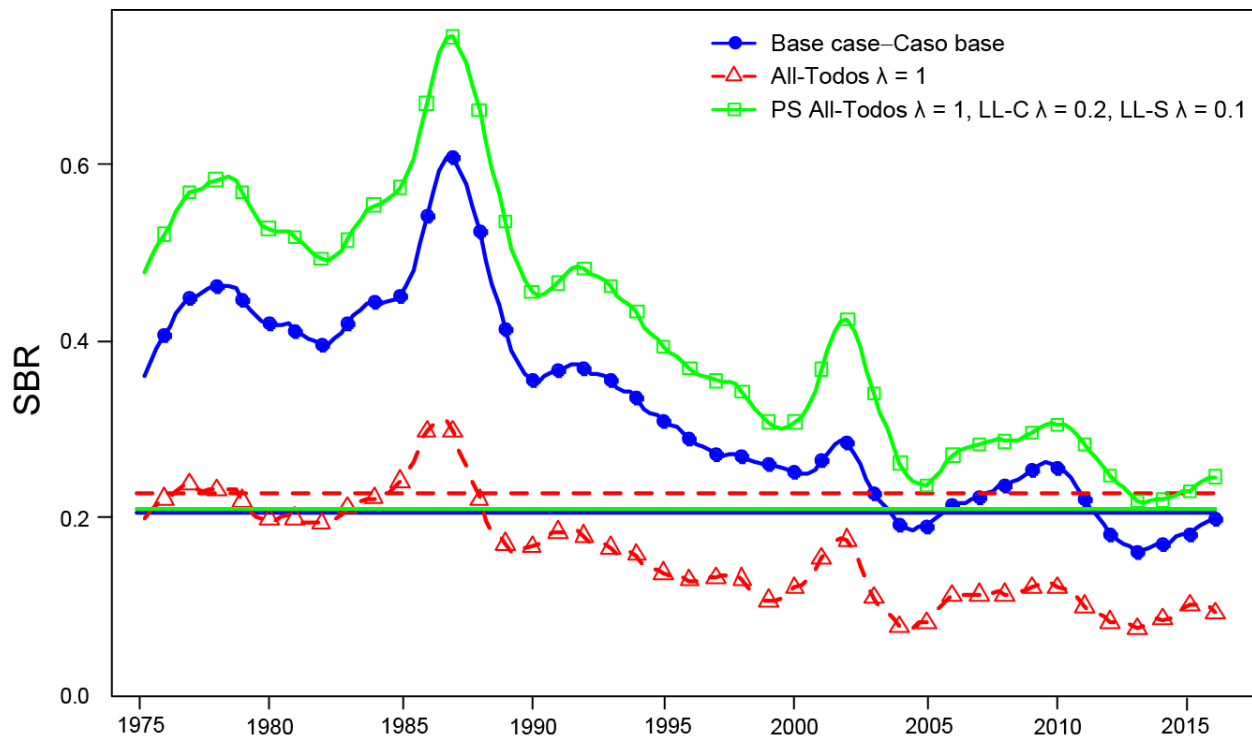


**FIGURE C.3.** Comparison of estimates of the spawning biomass ratio (SBR) of bigeye tuna from the base case analysis (blue dots;  $\lambda = 0.05$  for all fisheries) and two sensitivity analyses: 1) using the original input sample sizes of the size composition data of all fisheries ( $\lambda = 1$ , red triangles); 2) same as 1, except the logistic longline fisheries, whose size composition data are down-weighted (Fisheries 13-14;  $\lambda = 0.2$  and 0.1, respectively, green squares).

**FIGURA C.3.** Comparación de estimaciones del cociente de biomasa reproductora (SBR) de atún patudo del análisis de caso base (puntos azules;  $\lambda = 0.05$  para todas las pesquerías) y dos análisis de sensibilidad: 1) con el tamaño de muestra original de los datos de composición por talla de todas las pesquerías ( $\lambda = 1$ , triángulos rojos); 2) igual que 1, excepto las pesquerías palangreras logísticas con datos de composición por talla de ponderación reducida (Pesquerías 13-14;  $\lambda = 0.2$  y 0.1, respectivamente, cuadrados verdes).

**TABLE C.1.** Estimates of management-related quantities for bigeye tuna for the base case and for sensitivity analyses assigning different weighting factors ( $\lambda$ ) to the size-composition data for various fisheries.

**TABLA C.1.** Estimaciones de cantidades relacionadas con la ordenación del atún patudo del caso base y de los análisis de sensibilidad que asignan distintos factores de ponderación ( $\lambda$ ) a los datos de composición por talla de varias pesquerías.

|   | Base case-<br>Caso base | $\lambda = 1$ | F13: $\lambda = 0.2$<br>F14: $\lambda = 0.1$<br>Others/Otros: $\lambda = 1$ |
|---|-------------------------|---------------|---|
| MSY-RMS   | 107,864                 | 95,544        | 114,954   |
| $B_{\text{MSY}} - B_{\text{RMS}}$                                     | 389,211                 | 340,276       | 456,082   |
| $S_{\text{MSY}} - S_{\text{RMS}}$                                     | 95,101                  | 82,911        | 115,464   |
| $B_{\text{MSY}}/B_0 - B_{\text{RMS}}/B_0$                             | 0.26                    | 0.29          | 0.26  |
| $S_{\text{MSY}}/S_0 - S_{\text{RMS}}/S_0$                             | 0.21                    | 0.23          | 0.21  |
| $C_{\text{recent}}/\text{MSY} - C_{\text{recent}}/\text{RMS}$         | 0.97                    | 1.09          | 0.91  |
| $B_{\text{recent}}/B_{\text{MSY}} - B_{\text{recent}}/B_{\text{RMS}}$ | 1.00                    | 0.59          | 1.35  |
| $S_{\text{recent}}/S_{\text{MSY}} - S_{\text{recent}}/S_{\text{RMS}}$ | 0.96                    | 0.41          | 1.16  |
| $F$ multiplier-Multiplicador de $F$                                   | 1.05                    | 0.57          | 1.30  |

**APPENDIX D: SENSITIVITY ANALYSIS TO LOWER VALUES OF AVERAGE SIZE OF THE OLDEST FISH  
PARAMETER,  $L_2$**

**ANEXO D: ANÁLISIS DE SENSIBILIDAD A VALORES MENORES DEL PARÁMETRO DE TAMAÑO MEDIO DE LOS PECES MÁS VIEJOS,  $L_2$**

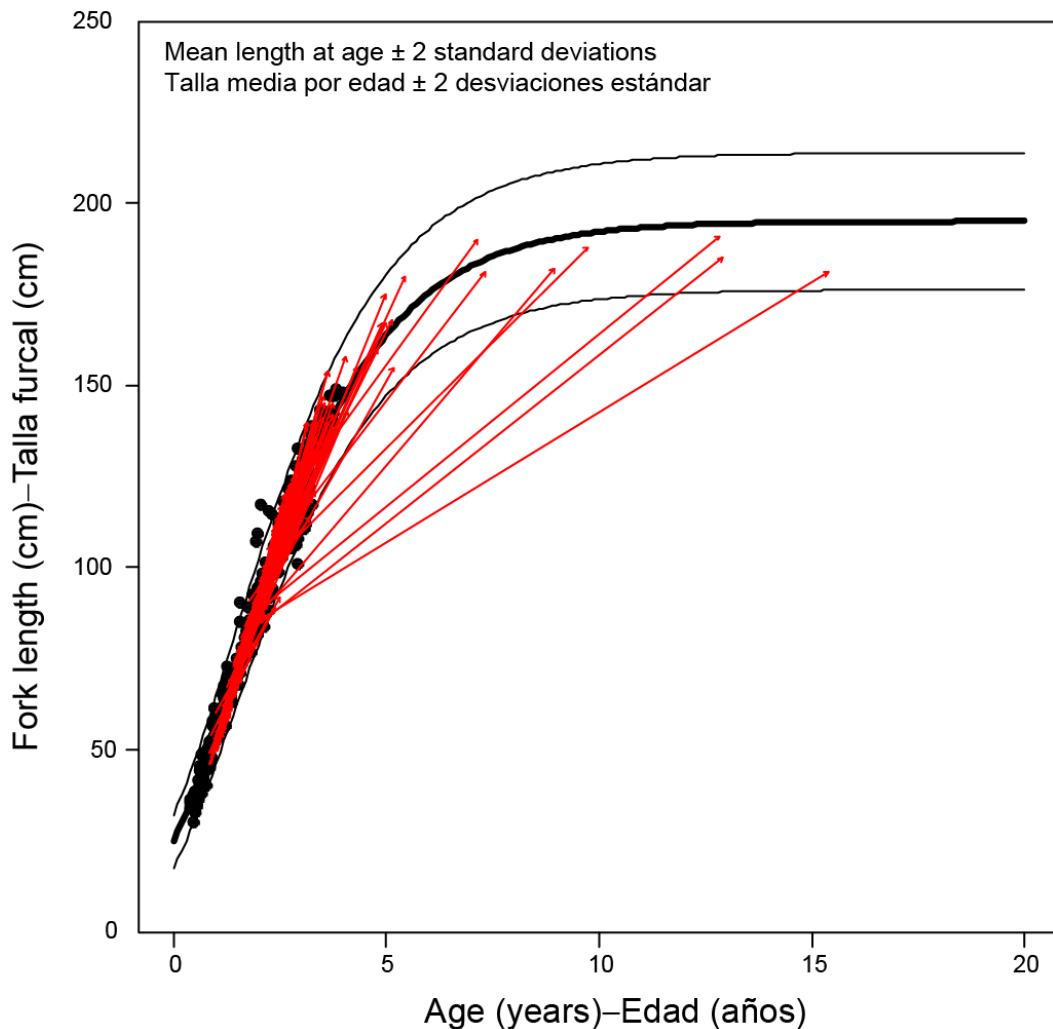


**FIGURE D.1.** Integrated growth model fitted to the two data components available for bigeye: black dots are age-at-length observations from otolith readings; red vectors link lengths at tag-release and tag-recapture. The growth curve is an update of Aires-da-Silva *et al.* (2015) to include three new observations, all with lengths at liberty above 10 years.

**FIGURA D.1.** Modelo integrado de crecimiento ajustado a los dos componentes de datos disponibles para el patudo: los puntos negros son observaciones de edad por talla de lecturas de otolitos; los vectores rojos conectan tallas de liberación y recaptura de marcas. La curva de crecimiento es una actualización de Aires-da-Silva *et al.* (2015) para incluir tres observaciones nuevas, todas con tiempos en libertad de más de 10 años

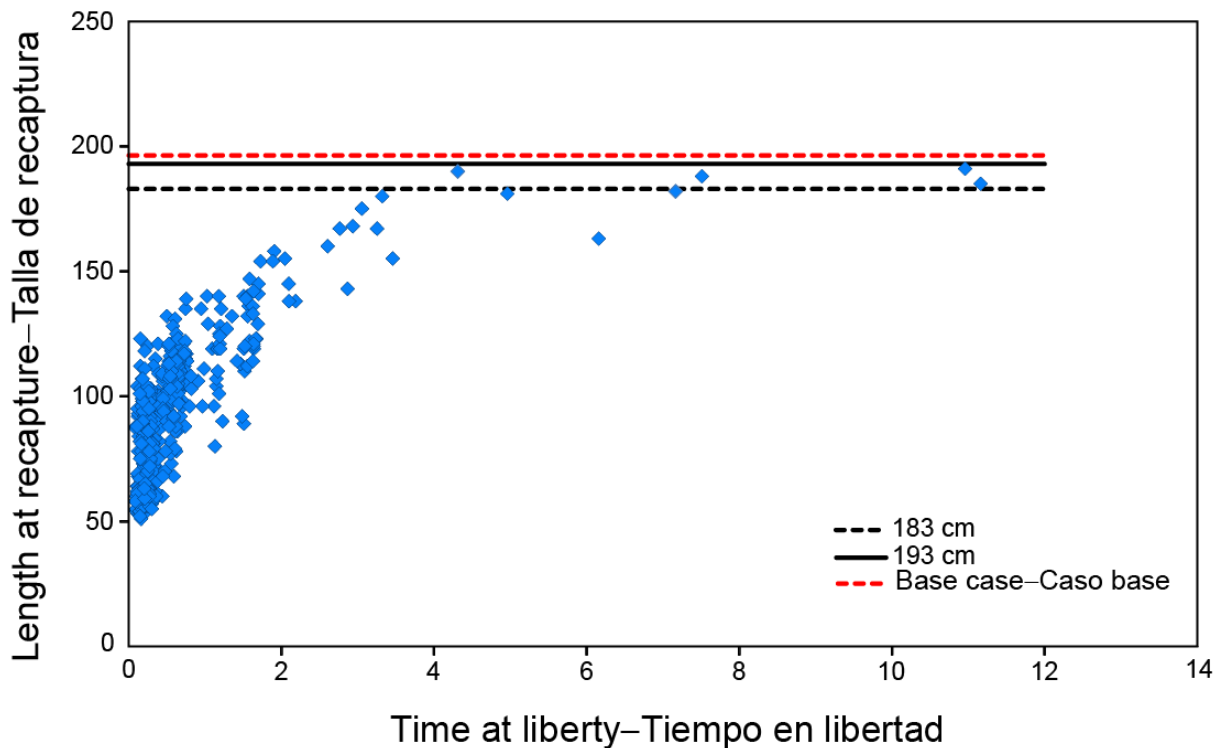


**FIGURE D.2.** Length at recapture of tagged bigeye against time at liberty. The horizontal dashed red line represents the  $L_2$  value fixed in the base case (196 cm, Aires-da-Silva *et al.* 2010). The solid and dashed black lines represent the lower  $L_2$  values assumed in two sensitivity analyses (196 and 183 cm).

**FIGURA D.2.** Talla de recaptura de patudos marcados como función de tiempo en libertad. La línea de trazos roja horizontal representa el valor de  $L_2$  fijado en el caso base (196 cm, Aires-da-Silva *et al.* 2010). Las líneas negras sólida y de trazos representan los valores de  $L_2$  más bajos supuestos en dos análisis de sensibilidad (196 y 183 cm).

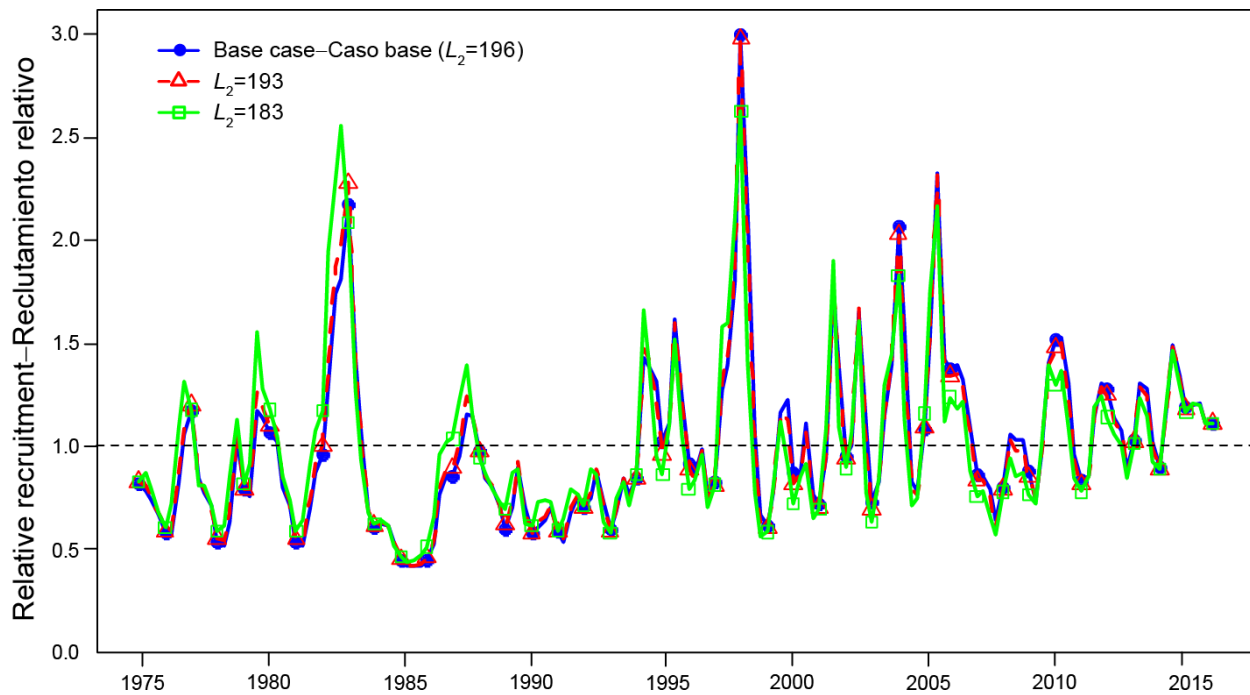


**FIGURE D.3a.** Comparison of estimates of relative recruitment for bigeye tuna from the base case analysis using a Richards growth curve with the average size of the oldest fish ( $L_2$ ) fixed at 196 cm (Aires-da-Silva *et al.* 2015), and two alternative models with  $L_2$  fixed at lower values (193 and 183 cm). The estimates are scaled so that the estimate of average recruitment is equal to 1.0 (dashed horizontal line).

**FIGURA D.3a.** Comparación de estimaciones del reclutamiento relativo de atún patudo del caso base, que usa a una curva de crecimiento de Richards con el tamaño medio de los peces más viejos fijado en 196 cm (Aires-da-Silva *et al.* 2015), y de dos modelos alternativos con  $L_2$  fijado en valores más bajos (193 y 183 cm). Se fija la escala de las estimaciones para que la estimación de reclutamiento medio equivalga a 1,0 (línea de trazos horizontal).

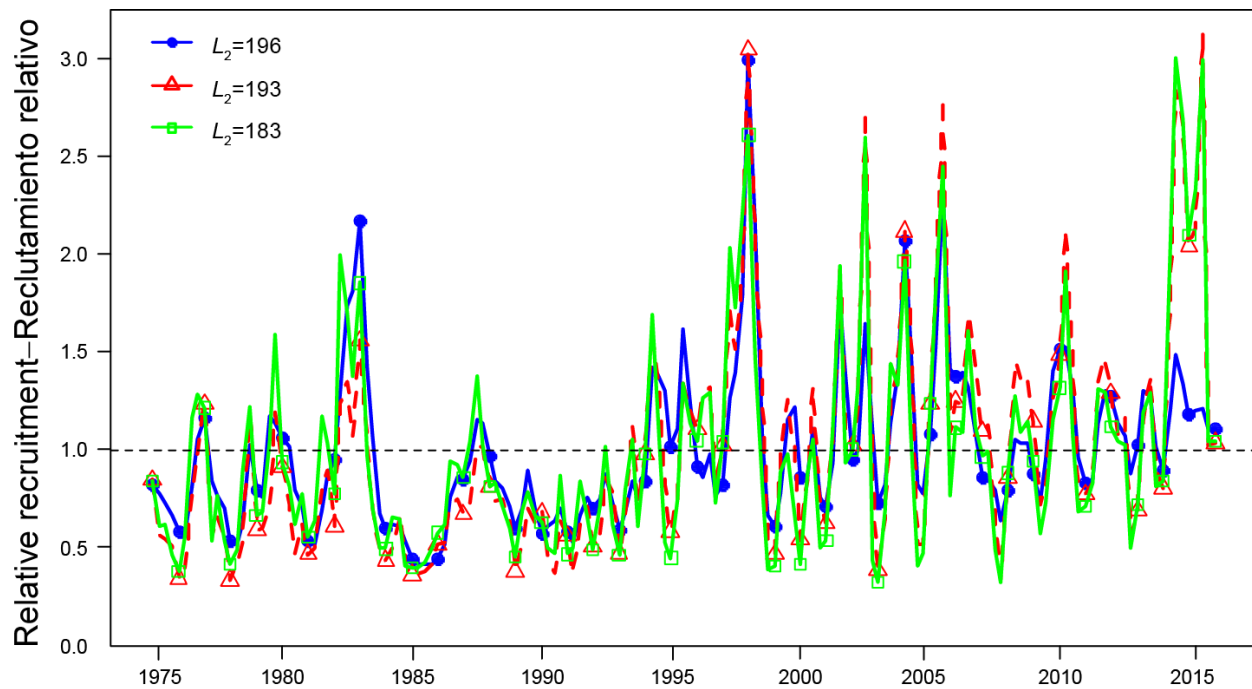


**FIGURE D.3b.** Comparison of estimates of relative recruitment for bigeye tuna from a model which, as in the base case, uses a Richards growth curve with the average size of the oldest fish ( $L_2$ ) fixed at 196 cm (Aires-da-Silva *et al.* 2015), and two alternative models with  $L_2$  fixed at lower values (193 and 183 cm). Unlike the base case, in which the size-composition data of all fisheries are down-weighted ( $\lambda = 0.05$ ), in these sensitivity analyses they are all up-weighted to their original sample sizes ( $\lambda = 1$ ). The estimates are scaled so that the estimate of average recruitment is equal to 1.0 (dashed horizontal line).

**FIGURA D.3b.** Comparación de estimaciones del reclutamiento relativo de atún patudo del caso base, que usa a una curva de crecimiento de Richards con el tamaño medio de los peces más viejos fijado en 196 cm (Aires-da-Silva *et al.* 2015), y de dos modelos alternativos, con  $L_2$  fijado en valores más bajos (193 y 183 cm). A diferencia del caso base, en el que se reduce la ponderación de los datos de composición por talla de todas las pesquerías ( $\lambda = 0.05$ ), en estos análisis de sensibilidad se incrementa su ponderación a sus tamaños de muestra originales ( $\lambda = 1$ ). Se fija la escala de las estimaciones para que la estimación de reclutamiento medio equivalga a 1,0 (línea de trazos horizontal).

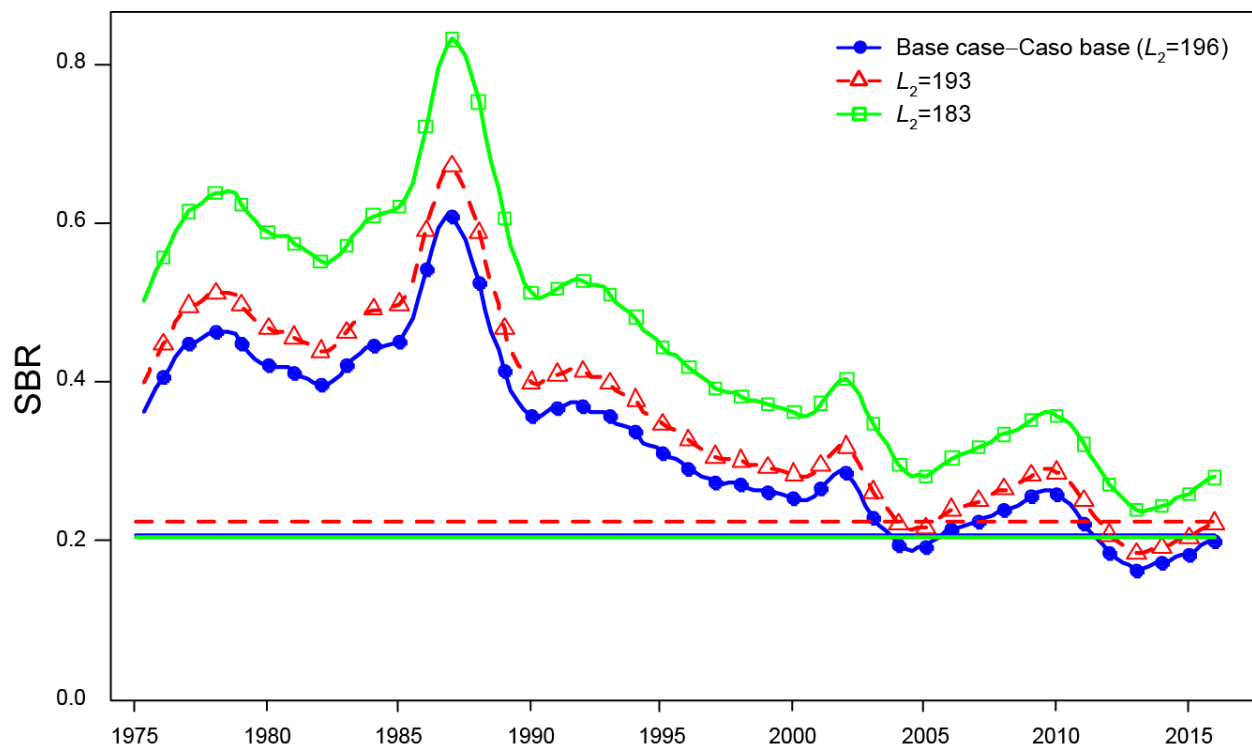


**FIGURE D.4a.** Comparison of estimates of the spawning biomass ratio (SBR) of bigeye tuna from a model which, as in the base case, uses a Richards growth curve with the average size of the oldest fish ( $L_2$ ) fixed at 196 cm (Aires-da-Silva *et al.* 2015), and two alternative models with  $L_2$  fixed at lower values (193 and 183 cm). The horizontal lines represent the SBRs associated with MSY in each scenario.

**FIGURA D.4a.** Comparación de estimaciones del cociente de biomasa reproductora (SBR) de atún patudo del caso base, que usa a una curva de crecimiento de Richards con el tamaño medio de los peces más viejos fijado en 196 cm (Aires-da-Silva *et al.* 2015), y de dos modelos alternativos, con  $L_2$  fijado en valores más bajos (193 y 183 cm). Las líneas horizontales representan los SBR asociados al RMS en cada escenario.

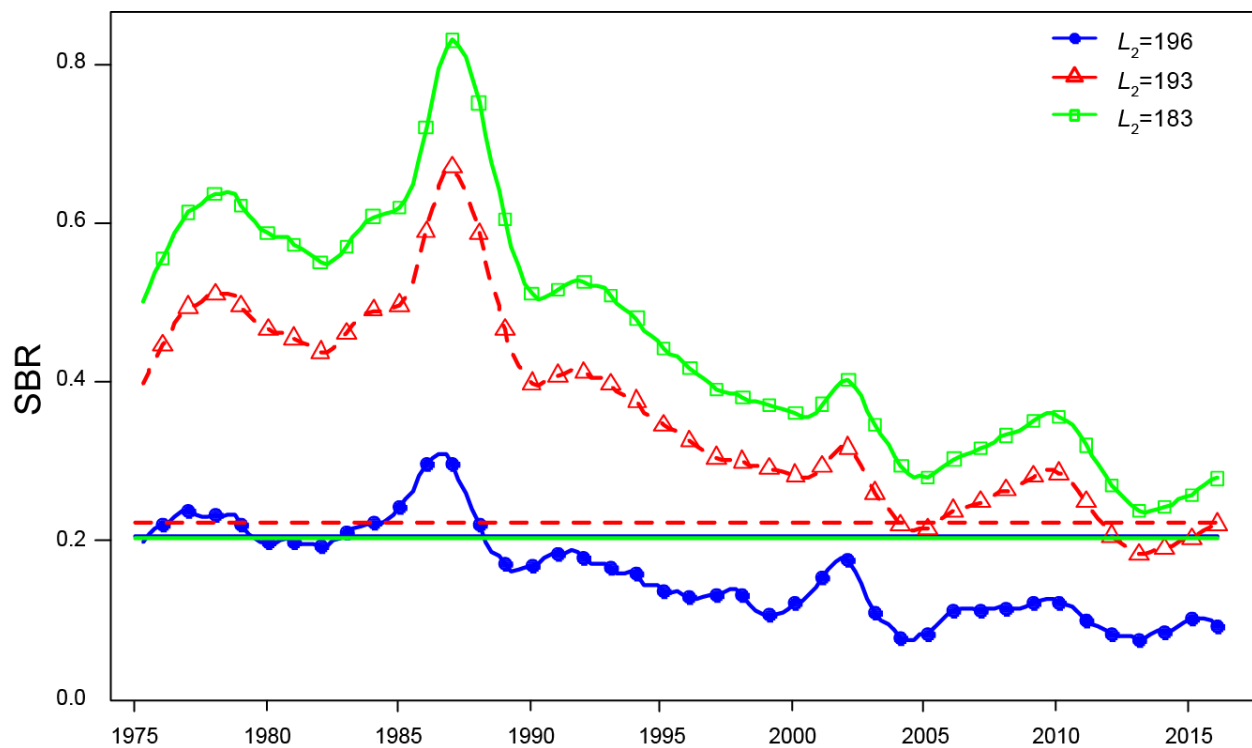


**FIGURE D.4b.** Comparison of estimates of the spawning biomass ratio (SBR) of bigeye tuna from a model which, as in the base case, uses a Richards growth curve with the average size of the oldest fish ( $L_2$ ) fixed at 196 cm (Aires-da-Silva *et al.* 2015), and two alternative models with  $L_2$  fixed at lower values (193 and 183 cm). Unlike in the base case, in which the size-composition data of all fisheries are down-weighted ( $\lambda = 0.05$ ), in these sensitivity analyses they are all up-weighted to their original sample sizes ( $\lambda = 1$ ). The horizontal lines represent the SBRs associated with MSY in each scenario.

**FIGURA D.4b.** Comparación de estimaciones del cociente de biomasa reproductora (SBR) de atún patudo de un modelo que, al igual que el caso base, usa una curva de crecimiento de Richards con el tamaño medio de los peces más viejos fijado en 196 cm (Aires-da-Silva *et al.* 2015), y dos modelos alternativos, con  $L_2$  fijado en valores más bajos (193 y 183 cm). A diferencia del caso base, en el que se reduce la ponderación de los datos de composición por talla de todas las pesquerías ( $\lambda = 0.05$ ), en estos análisis de sensibilidad se incrementa su ponderación a sus tamaños de muestra originales ( $\lambda = 1$ ). Las líneas horizontales representan los SBR asociados al RMS en cada escenario.

**TABLE D.1.** Estimates of management-related quantities for bigeye tuna for the base case and the sensitivity analysis to the average size of the oldest fish ( $L_2$ ). Unlike in the base case and the first two analyses of sensitivity to lower values of  $L_2$  (193 and 183 cm), in which the size-composition data of all fisheries are down-weighted ( $\lambda = 0.05$ ), in the last three sensitivity analyses they are all up-weighted to their original sample sizes ( $\lambda = 1$ ).

**TABLA D.1.** Estimaciones de las cantidades relacionadas con la ordenación para el atún patudo del caso base y del análisis de sensibilidad al tamaño medio de los peces más viejos ( $L_2$ ). A diferencia del caso base y los dos primeros análisis de sensibilidad a valores menores de  $L_2$  (193 y 183 cm), en los que se reduce la ponderación de los datos de composición por talla de todas las pesquería ( $\lambda = 0.05$ ), en los tres últimos análisis de sensibilidad se incrementa su ponderación al tamaño original de muestra ( $\lambda = 1$ ).

|   | Base case-<br>Caso base | $\lambda = 0.05$ | $\lambda = 0.05$ | $\lambda = 1$ | $\lambda = 1$ | $\lambda = 1$ |
|---|-------------------------|------------------|------------------|---------------|---------------|---------------|
| $L_2$   | 196                     | 193              | 183              | 196           | 193           | 183           |
| MSY-RMS   | 107,864                 | 110,115          | 120,434          | 95,544        | 100,872       | 107,620       |
| $B_{\text{MSY}} - B_{\text{RMS}}$                                     | 389,211                 | 399,907          | 432,280          | 340,276       | 352,365       | 382,856       |
| $S_{\text{MSY}} - S_{\text{RMS}}$                                     | 95,101                  | 94,726           | 90,508           | 82,911        | 81,834        | 79,086        |
| $B_{\text{MSY}}/B_0 - B_{\text{RMS}}/B_0$                             | 0.26                    | 0.26             | 0.25             | 0.29          | 0.29          | 0.27          |
| $S_{\text{MSY}}/S_0 - S_{\text{RMS}}/S_0$                             | 0.21                    | 0.21             | 0.19             | 0.23          | 0.22          | 0.2           |
| $C_{\text{recent}}/\text{MSY} - C_{\text{recent}}/\text{RMS}$         | 0.97                    | 0.95             | 0.87             | 1.09          | 1.03          | 0.97          |
| $B_{\text{recent}}/B_{\text{MSY}} - B_{\text{recent}}/B_{\text{RMS}}$ | 1.00                    | 1.11             | 1.39             | 0.59          | 0.77          | 1.29          |
| $S_{\text{recent}}/S_{\text{MSY}} - S_{\text{recent}}/S_{\text{RMS}}$ | 0.96                    | 1.08             | 1.45             | 0.41          | 0.53          | 1.06          |
| $F$ multiplier-Multiplicador de $F$                                   | 1.05                    | 1.16             | 1.53             | 0.57          | 0.69          | 1.16          |

**APPENDIX E: SENSITIVITY ANALYSIS TO HIGHER RATES OF JUVENILE NATURAL MORTALITY**  
**ANEXO E: ANÁLISIS DE SENSIBILIDAD A TASAS MAYORES DE MORTALIDAD NATURAL DE JUVENILES**

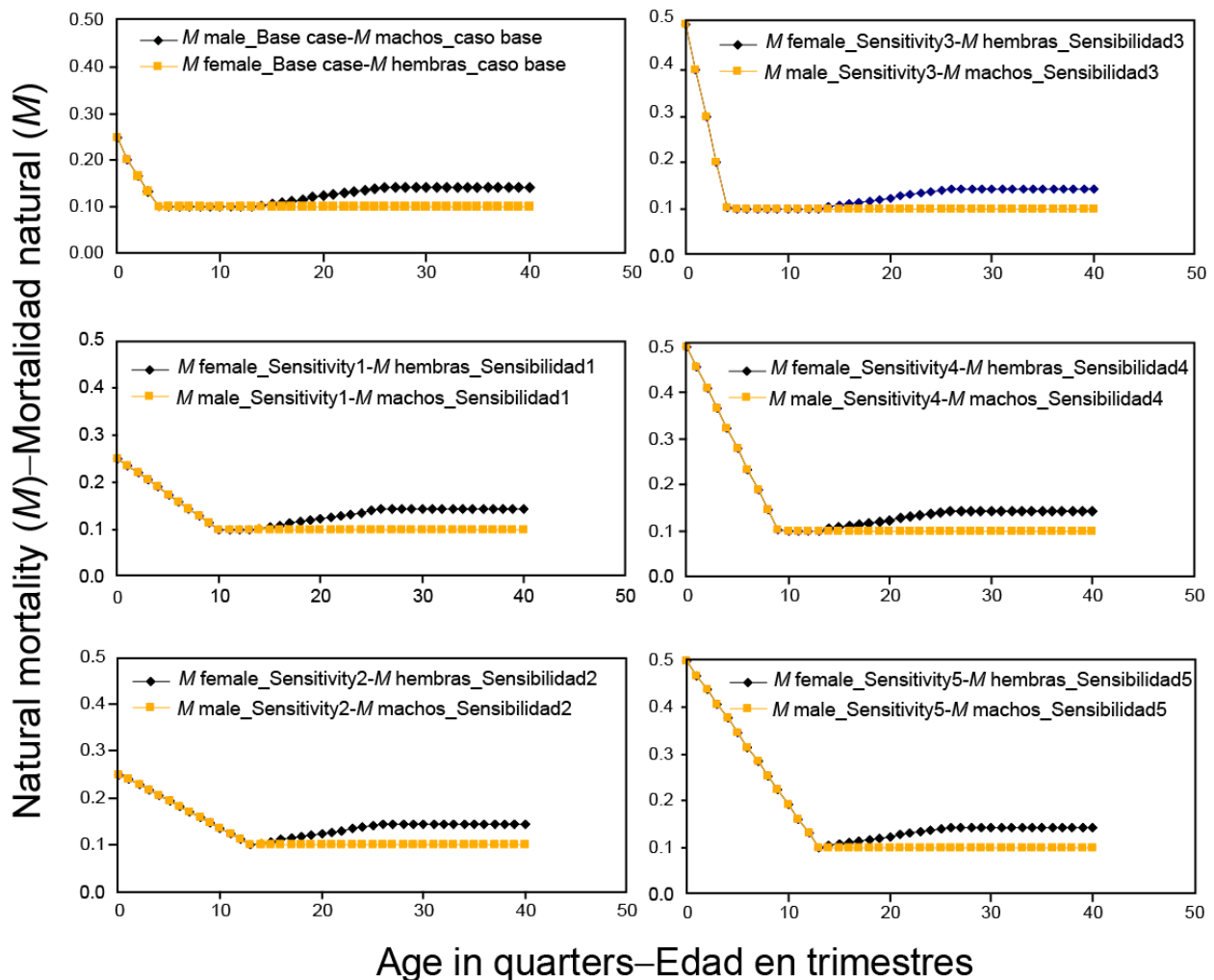


**FIGURE E.1.** Natural mortality ( $M$ ) curves for female and male bigeye tuna investigated in the analyses of sensitivity to higher rates of juvenile natural mortality.

**FIGURA E.1.** Curvas de mortalidad natural ( $M$ ) de atunes patudo macho y hembra investigadas en los análisis de sensibilidad a tasas mayores de mortalidad natural juvenil.

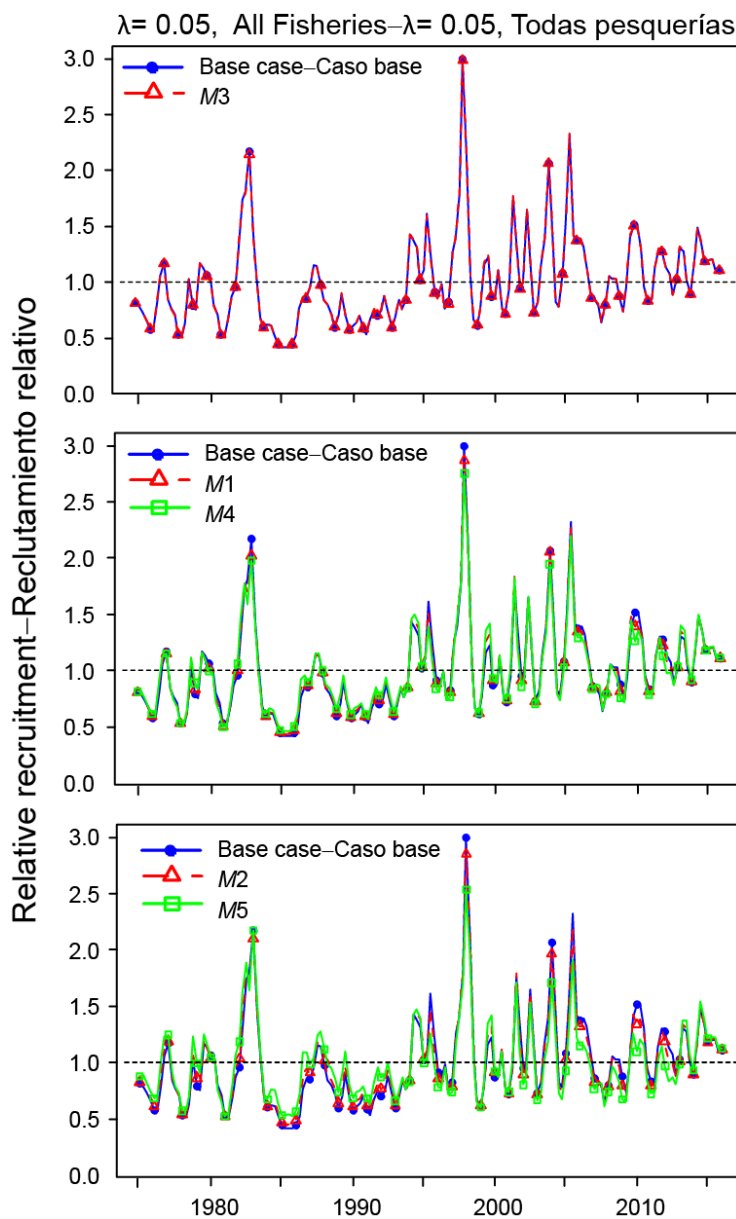


**FIGURE E.2a.** Comparison of estimates of relative recruitment for bigeye tuna from the base case analysis and from sensitivity analyses assuming rates of juvenile natural mortality ( $M$ ) (see Figure E.1 to compare  $M$  schedules). The sensitivity analyses assumed the same weighting of the size-composition data as in the base case ( $\lambda = 0.05$ ). The estimates are scaled so that the estimate of average recruitment is equal to 1.0 (dashed horizontal line).

**FIGURA E.2a.** Comparación de las estimaciones de reclutamiento relativo de atún patudo del análisis de caso base y de los análisis de sensibilidad que suponen tasas de mortalidad natural ( $M$ ) juvenil (ver Figura E.1 para comparar vectores de  $M$ ). Los análisis de sensibilidad suponen la misma ponderación de los datos de composición por talla que en el caso base ( $\lambda = 0.05$ ). Se fija la escala de las estimaciones para que la estimación de reclutamiento medio equivalga a 1,0 (línea de trazos horizontal).

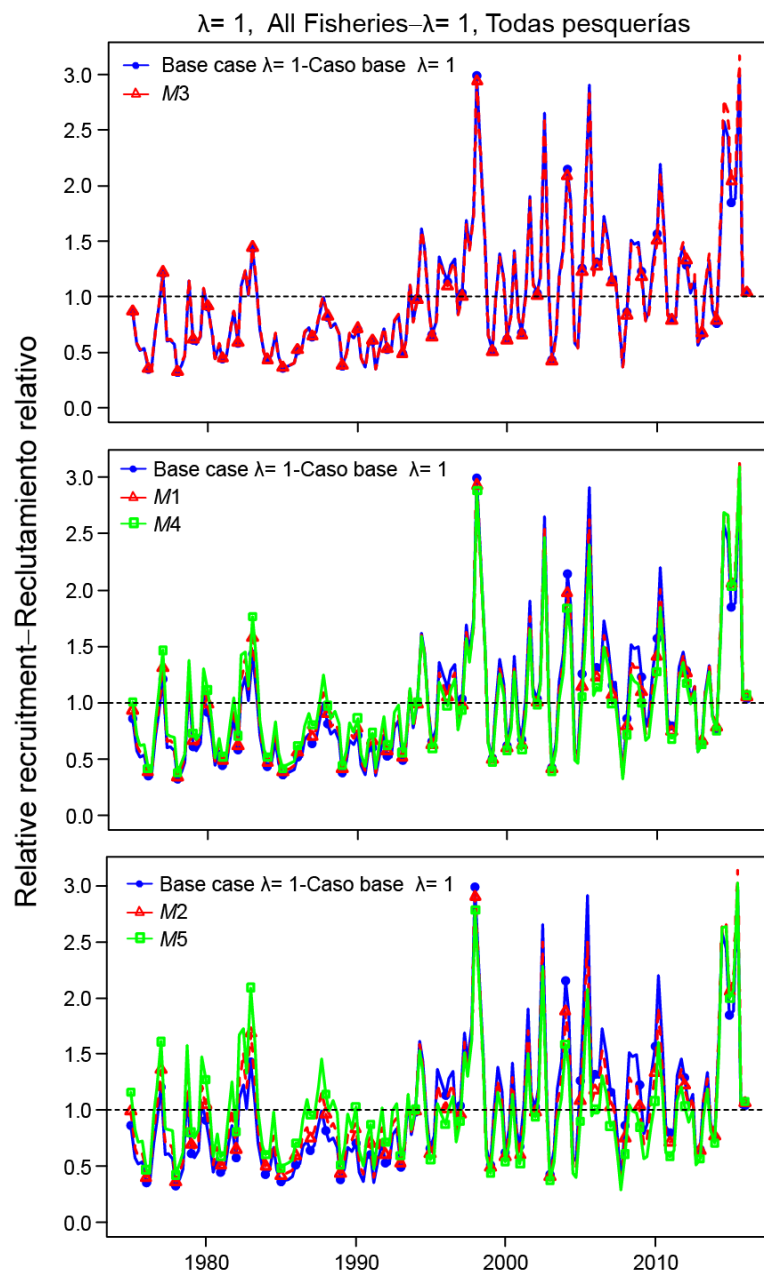


**FIGURE E.2b.** Comparison of estimates of relative recruitment for bigeye tuna from a base case configuration model (except  $\lambda = 1$  for all size-composition data) and from sensitivity analyses with various rates of juvenile natural mortality ( $M$ ) (see Figure E.1 to compare  $M$  schedules). The estimates are scaled so that the estimate of average recruitment is equal to 1.0 (dashed horizontal line).

**FIGURA E.2b.** Comparación de las estimaciones de reclutamiento relativo de atún patudo de un modelo con configuración de caso base (excepto que  $\lambda = 1$  para todos los datos de composición por talla) y de análisis de sensibilidad con varias tasas de mortalidad natural ( $M$ ) juvenil (ver Figura E.1 para comparar vectores de  $M$ ). Se fija la escala de las estimaciones para que la estimación de reclutamiento medio equivalga a 1,0 (línea de trazos horizontal).

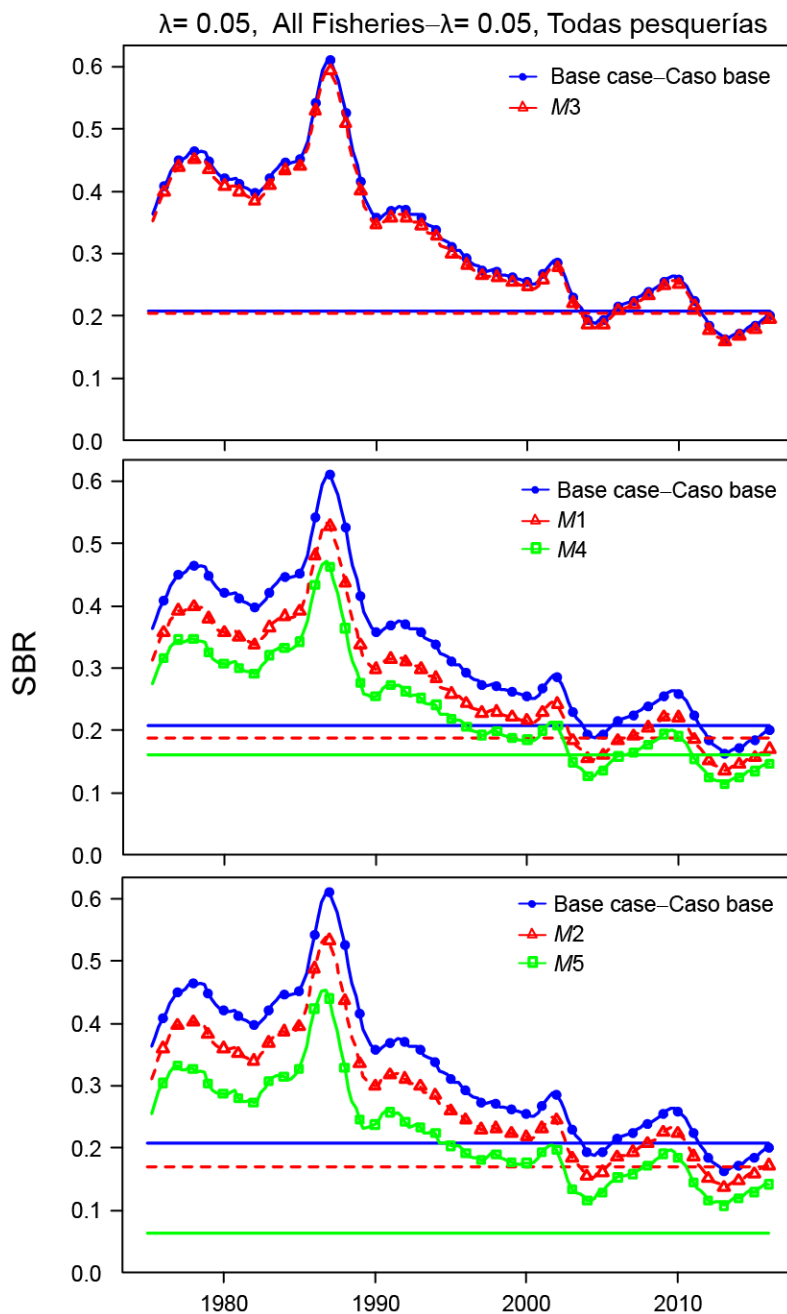


**FIGURE E.3a.** Comparison of estimates of the spawning biomass ratio (SBR) for bigeye tuna from the base case analysis and from sensitivity analyses with various rates of juvenile natural mortality ( $M$ ) (see Figure E.1 to compare  $M$  schedules). The sensitivity analyses assumed the same weighting of the size composition data as in the base case ( $\lambda = 0.05$ ). The horizontal lines represent the SBRs associated with MSY in each scenario.

**FIGURA E.3a.** Comparación de las estimaciones del cociente de biomasa reproductora (SBR) del análisis de caso base y de análisis de sensibilidad con varias tasas de mortalidad natural ( $M$ ) juvenil (ver Figura E.1 para comparar vectores de  $M$ ). Los análisis de sensibilidad suponen la misma ponderación de los datos de composición por talla que en el caso base ( $\lambda = 0.05$ ). Las líneas horizontales representan los SBR asociados al RMS en cada escenario.

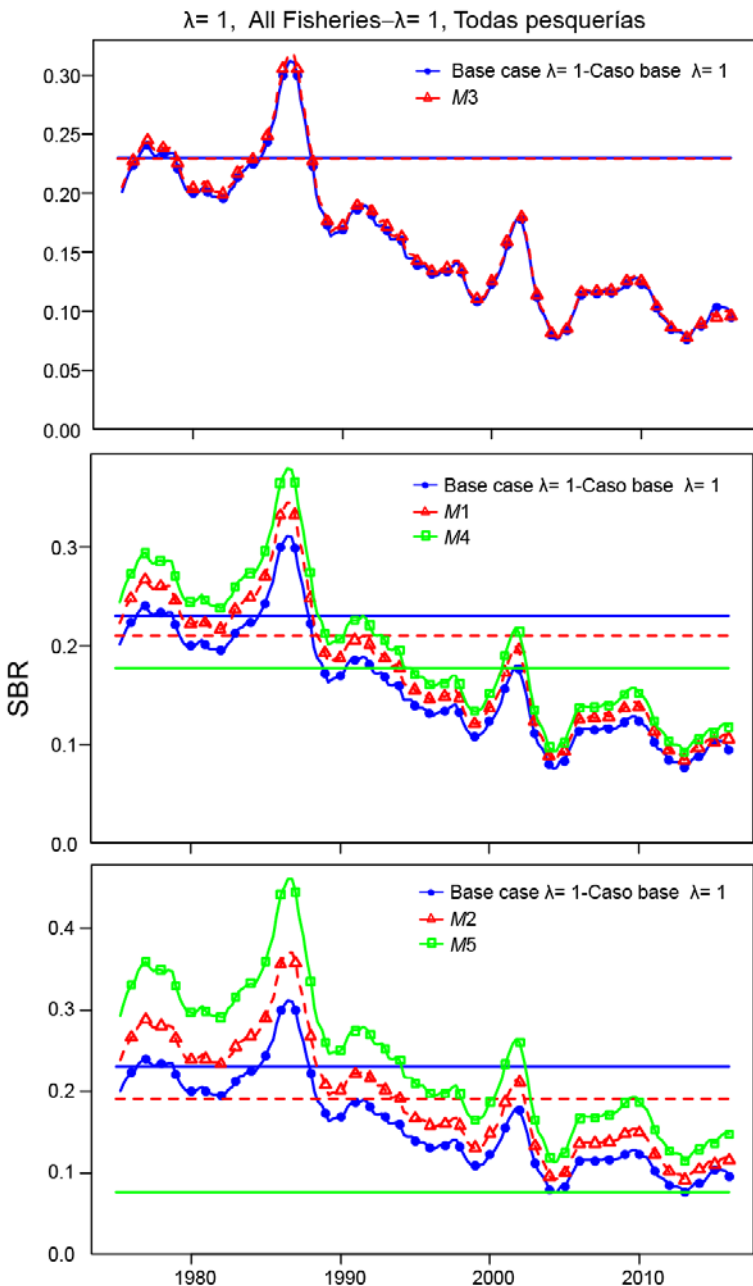


**FIGURE E.3b.** Comparison of estimates of the spawning biomass ratio (SBR) for bigeye tuna from a base case configuration model (except  $\lambda = 1$  for all size composition data) and from sensitivity analyses with various rates of juvenile natural mortality ( $M$ ) (see Figure E.1 to compare  $M$  schedules).. The horizontal lines represent the SBRs associated with MSY in each scenario.

**FIGURA E.3b.** Comparación de las estimaciones del cociente de biomasa reproductora (SBR) de un modelo con configuración de caso base (excepto que  $\lambda = 1$  para todos los datos de composición por talla) y de análisis de sensibilidad con varias tasas de mortalidad natural ( $M$ ) juvenil (ver Figura E.1 para comparar vectores de  $M$ ). Las líneas horizontales representan los SBR asociados al RMS en cada escenario.

**TABLE E.1.** Estimates of management-related quantities for bigeye tuna for the base case and the sensitivity analysis to higher values of juvenile natural mortality ( $M_0$ ). The sensitivity analyses were conducted assuming one of two values of  $M_0$  (0.25 and 0.50 quarter $^{-1}$ ), and a linear decreasing trend of  $M$  between age-0 and one of three possible young ages (5, 10 and 13 quarters) (see Figure E.1 to compare  $M$  schedules). The sensitivity analyses were done for both data-weighting configurations of the size-composition data ( $\lambda = 0.05$  for all fisheries, as in the base case, and with the original sample sizes for all fisheries,  $\lambda = 1$ ).

**TABLA E.1.** Estimaciones de cantidades relacionadas con la ordenación del patudo correspondientes al caso base y al análisis de sensibilidad a valores mayores de mortalidad natural  $M_0$  juvenil. Se realizaron los análisis de sensibilidad con uno de dos valores de  $M_0$  (0.25 y 0.50 trimestre $^{-1}$ ), y una tendencia lineal decreciente de  $M$  entre edad 0 y una de tres edades jóvenes posibles (5, 10 y 13 trimestres) (ver Figura E.1 para comparar vectores de  $M$ ). Se realizaron los análisis de sensibilidad para ambas configuraciones de ponderación de los datos de composición por talla ( $\lambda = 0.05$  para todas las pesquerías, al igual que en el caso base, y con el tamaño de muestra original para todas las pesquerías,  $\lambda = 1$ ).

| $\lambda = 0.05$ , all fisheries—<br>todas pesquerías                 | $M_0 = 0.25$ | $M_0 = 0.5$ | $M_0 = 0.25$ | $M_0 = 0.5$ | $M_0 = 0.25$ | $M_0 = 0.5$ |
|---|--------------|-------------|--------------|-------------|--------------|-------------|
| Age (quarters)<br>Edad (trimestres)                                   | 5            | 5           | 10           | 10          | 13           | 13          |
| MSY-RMS   | 107,864      | 107,692     | 108,830      | 111,450     | 112,312      | 126,262     |
| $B_{\text{MSY}} - B_{\text{RMS}}$                                     | 389,211      | 374,742     | 326,723      | 281,092     | 305,120      | 211,981     |
| $S_{\text{MSY}} - S_{\text{RMS}}$                                     | 95,101       | 90,427      | 71,794       | 52,902      | 60,632       | 16,596      |
| $B_{\text{MSY}}/B_0 - B_{\text{RMS}}/B_0$                             | 0.26         | 0.26        | 0.26         | 0.26        | 0.25         | 0.22        |
| $S_{\text{MSY}}/S_0 - S_{\text{RMS}}/S_0$                             | 0.21         | 0.21        | 0.19         | 0.16        | 0.17         | 0.064       |
| $C_{\text{recent}}/\text{MSY} - C_{\text{recent}}/\text{RMS}$         | 0.97         | 0.97        | 0.96         | 0.94        | 0.93         | 0.83        |
| $B_{\text{recent}}/B_{\text{MSY}} - B_{\text{recent}}/B_{\text{RMS}}$ | 1.00         | 0.99        | 0.97         | 1.00        | 1.06         | 1.55        |
| $S_{\text{recent}}/S_{\text{MSY}} - S_{\text{recent}}/S_{\text{RMS}}$ | 0.96         | 0.95        | 0.9          | 0.91        | 1.01         | 2.22        |
| $F$ multiplier-   |              |             |              |             |              |             |
| Multiplicador de $F$  | 1.05         | 1.04        | 1.01         | 1.03        | 1.11         | 1.77        |
| $\lambda = 1$ , all fisheries—<br>todas pesquerías                    | $M_0 = 0.25$ | $M_0 = 0.5$ | $M_0 = 0.25$ | $M_0 = 0.5$ | $M_0 = 0.25$ | $M_0 = 0.5$ |
| Age (quarters)<br>Edad (trimestres)                                   | 5            | 5           | 10           | 10          | 13           | 13          |
| MSY-RMS   | 95,544       | 102,822     | 105,136      | 109,484     | 107,477      | 126,703     |
| $B_{\text{MSY}} - B_{\text{RMS}}$                                     | 340,276      | 345,811     | 319,633      | 286,226     | 301,285      | 225,595     |
| $S_{\text{MSY}} - S_{\text{RMS}}$                                     | 82,911       | 82,195      | 70,235       | 54,692      | 60,012       | 19,854      |
| $B_{\text{MSY}}/B_0 - B_{\text{RMS}}/B_0$                             | 0.29         | 0.3         | 0.29         | 0.28        | 0.28         | 0.23        |
| $S_{\text{MSY}}/S_0 - S_{\text{RMS}}/S_0$                             | 0.23         | 0.23        | 0.21         | 0.18        | 0.19         | 0.076       |
| $C_{\text{recent}}/\text{MSY} - C_{\text{recent}}/\text{RMS}$         | 1.09         | 1.01        | 0.99         | 0.95        | 0.97         | 0.82        |
| $B_{\text{recent}}/B_{\text{MSY}} - B_{\text{recent}}/B_{\text{RMS}}$ | 0.59         | 0.66        | 0.81         | 1.03        | 0.94         | 1.88        |
| $S_{\text{recent}}/S_{\text{MSY}} - S_{\text{recent}}/S_{\text{RMS}}$ | 0.41         | 0.42        | 0.51         | 0.66        | 0.6          | 1.93        |
| $F$ multiplier-   |              |             |              |             |              |             |
| Multiplicador de $F$  | 0.57         | 0.59        | 0.68         | 0.84        | 0.78         | 1.7         |

**APPENDIX F: SENSITIVITY ANALYSIS TO LOWER AND HIGHER RATES OF ADULT NATURAL MORTALITY**  
**ANEXO F: ANÁLISIS DE SENSIBILIDAD A TASAS MAYORES Y MENORES DE MORTALIDAD NATURAL DE ADULTOS**

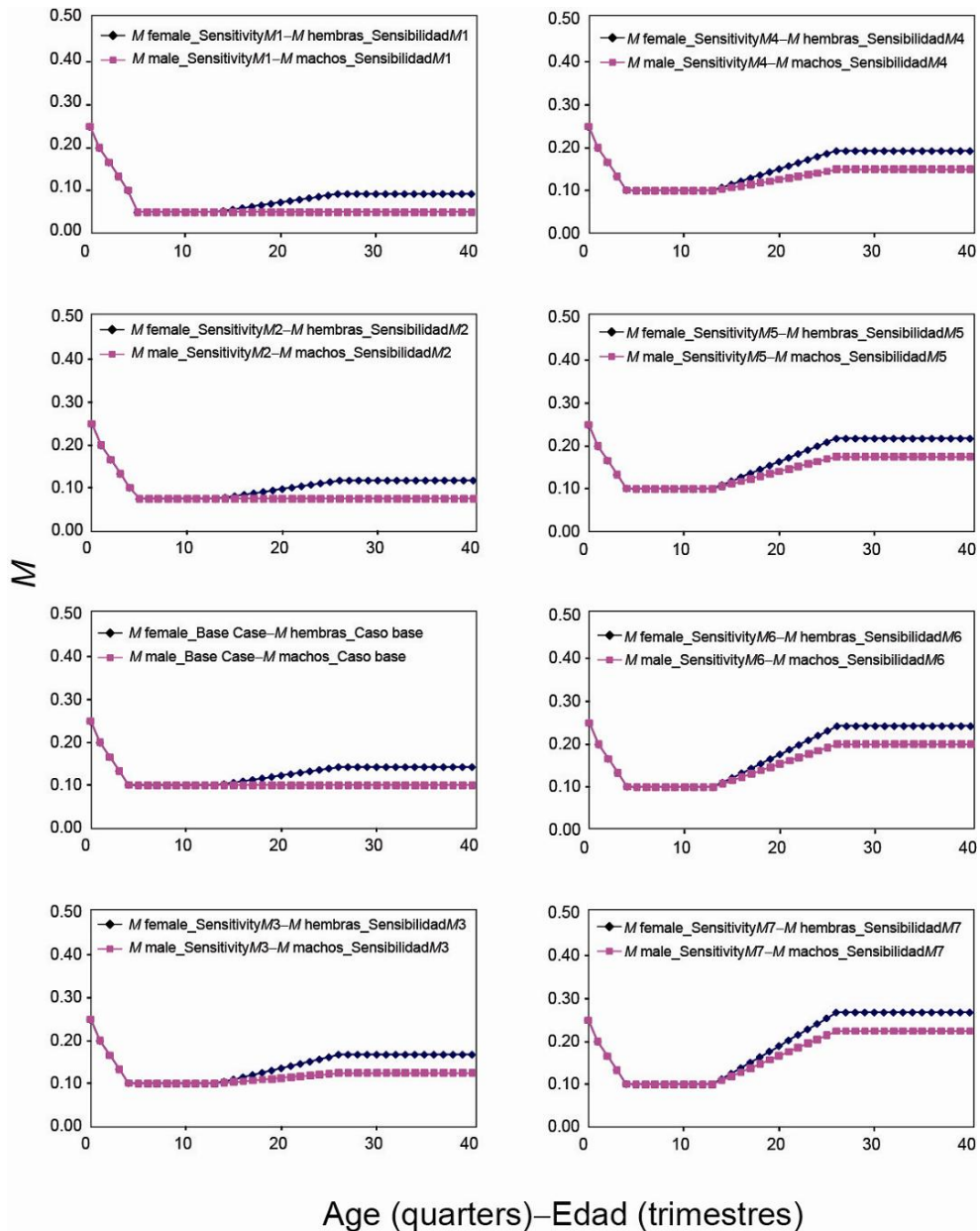


**FIGURE F.1.** Natural mortality ( $M$ ) schedules for female and male bigeye investigated in the sensitivity analysis to lower and higher  $M$  values for adults.

**FIGURA F.1.** Vectores de mortalidad natural ( $M$ ) de patudos hembra y macho investigados en el análisis de sensibilidad a valores mayores y menores de  $M$  para los adultos.

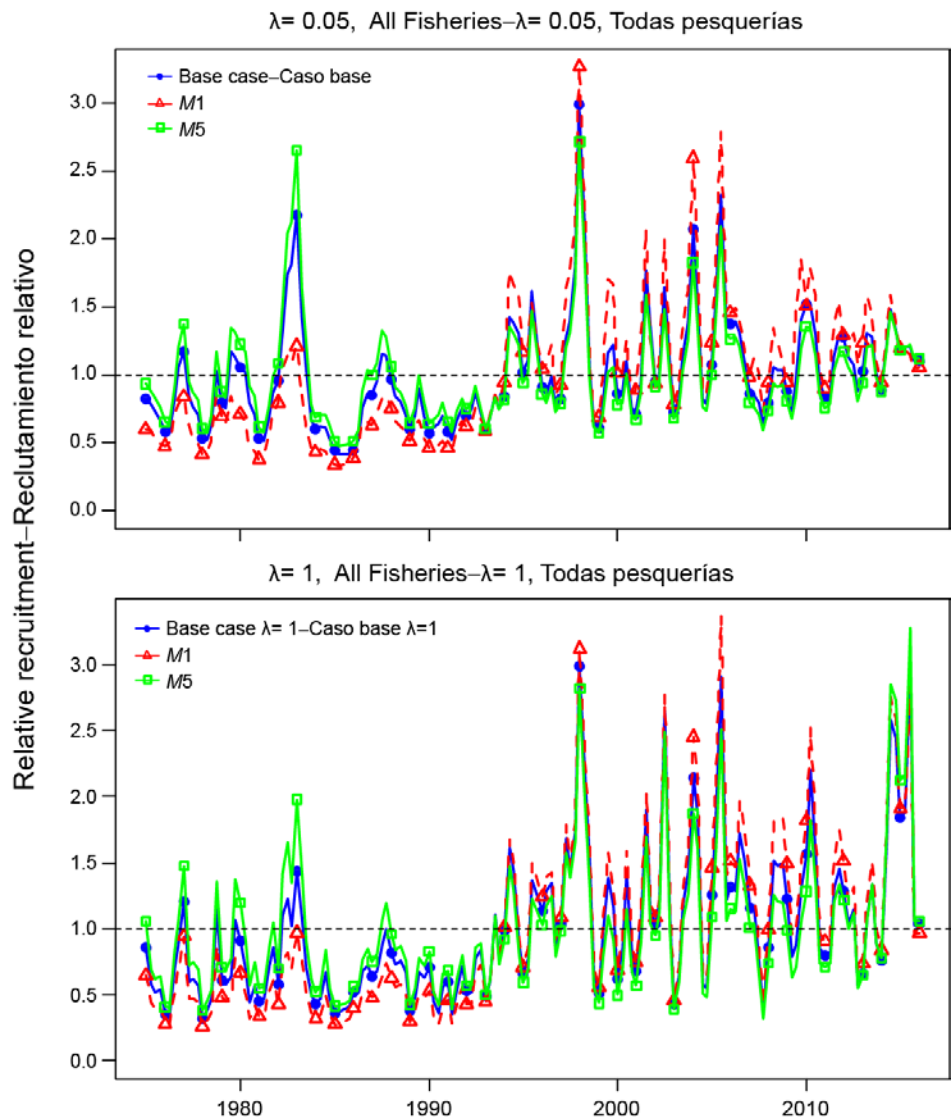


**FIGURE F.2.** Comparison of estimates of relative recruitment of bigeye tuna from the base case analysis and from two sensitivity analyses assuming lower ( $M_1$ ) and higher ( $M_5$ ) rates of adult natural mortality ( $M$ ) (see Figure F.1 to compare  $M$  schedules). The estimates are scaled so that the estimate of average recruitment is equal to 1.0 (dashed horizontal line). The sensitivity analyses were conducted for two weighting scenarios for the size-composition data: a) same weighting as in the base case ( $\lambda = 0.05$  for all fisheries) (upper panel); b) original sample sizes for all fisheries ( $\lambda = 1$ ) (lower panel).

**FIGURA F.2.** Comparación de estimaciones del reclutamiento relativo de atún patudo del análisis de caso base y de dos análisis de sensibilidad que suponen tasas de mortalidad natural ( $M$ ) adulta más bajas ( $M_1$ ) y más altas ( $M_5$ ) (ver Figura F.1 para comparar vectores de  $M$ ). Se fija la escala de las estimaciones para que la estimación de reclutamiento medio equivalga a 1,0 (línea de trazos horizontal). Se realizaron análisis de sensibilidad con dos escenarios de ponderación para los datos de composición por tamaño: a) misma ponderación que en el caso base ( $\lambda = 0.05$  para todas las pesquerías) (recuadro superior); b) tamaño de muestra original para todas las pesquerías ( $\lambda = 1$ ) (recuadro inferior).

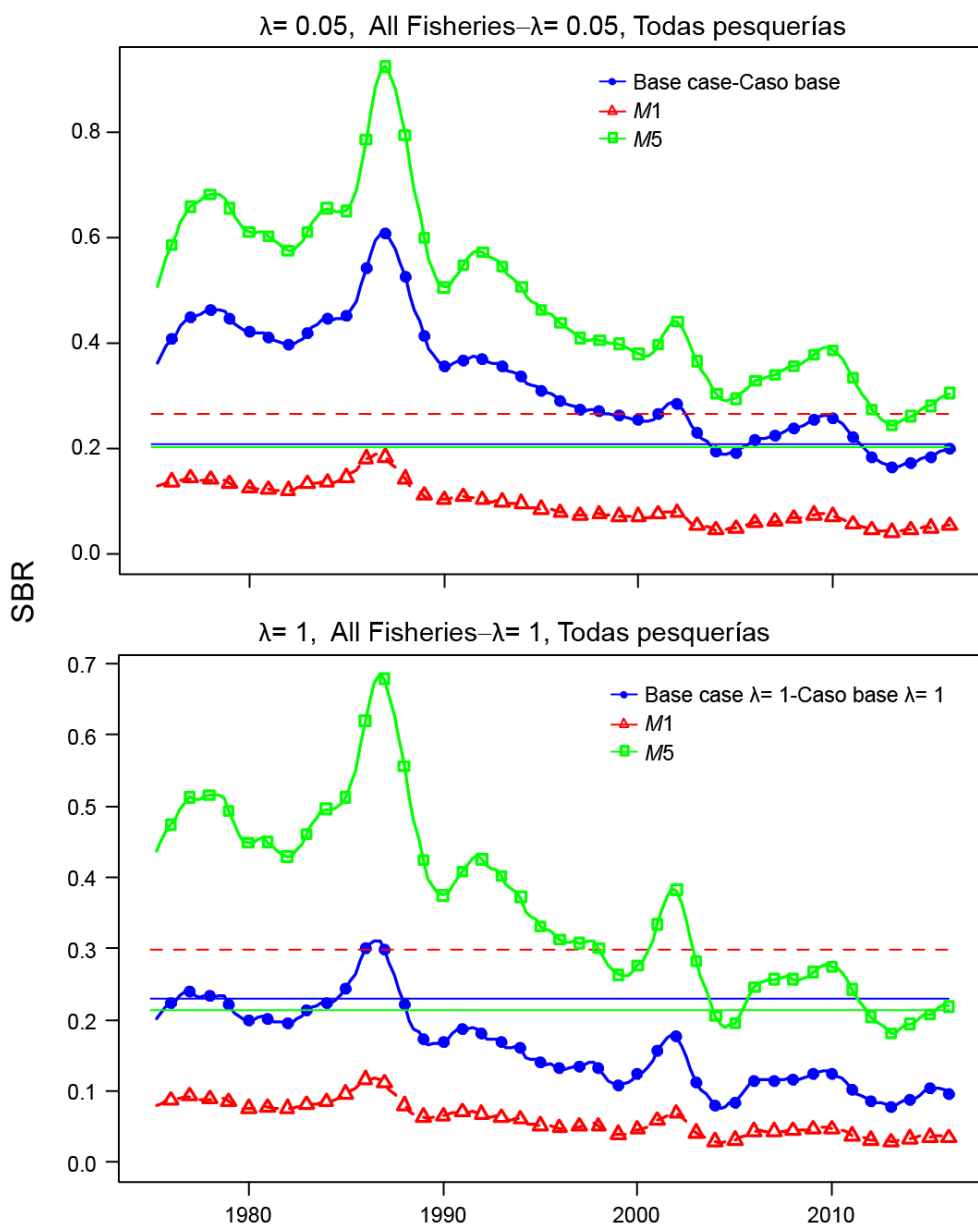


**FIGURE F.3.** Comparison of estimates of the spawning biomass ratio (SBR) of bigeye tuna from the base case analysis and from two sensitivity analyses assuming lower ( $M_1$ ) and higher ( $M_5$ ) rates of adult natural mortality ( $M$ ) (see Figure F.1 to compare  $M$  schedules). The horizontal lines represent the SBRs associated with MSY in each scenario. The sensitivity analyses were conducted for two weighting scenarios for the size-composition data: a) same weighting as in the base case ( $\lambda = 0.05$  for all fisheries) (upper panel); b) original sample sizes for all fisheries ( $\lambda = 1$ ) (lower panel).

**FIGURA F.3.** Comparación de las estimaciones del cociente de biomasa reproductora (SBR) del análisis de caso base y de análisis de sensibilidad que suponen tasas de mortalidad natural ( $M$ ) adulta más bajas ( $M_1$ ) y más altas ( $M_5$ ) (ver Figura F.1 para comparar vectores de  $M$ ). Las líneas horizontales representan los SBR asociados al RMS en cada escenario. Se realizaron los análisis de sensibilidad con dos escenarios de ponderación para los datos de composición por tamaño: a) misma ponderación que en el caso base ( $\lambda = 0.05$  para todas las pesquerías) (recuadro superior); b) tamaño de muestra original para todas las pesquerías ( $\lambda = 1$ ) (recuadro inferior).

**TABLE F.1.** Estimates of management-related quantities for bigeye tuna for the base case and adult natural mortality ( $M$ ) sensitivity analysis (see Figure F.1 to compare  $M$  schedules).

**TABLA F.1.** Estimaciones de las cantidades relacionadas con la ordenación para el atún patudo del caso base y del análisis de sensibilidad a la mortalidad natural ( $M$ ) de adultos (ver Figura F.1 para comparar vectores de  $M$ ).

| $\lambda = 0.05$ , all fisheries—<br>todas pesquerías                 | <b>Mad-sens1</b> | <b>Mad-sens2</b> | <b>Base<br/>case<br/>Caso<br/>base</b> | <b>Mad-sens3</b> | <b>Mad-sens4</b> | <b>Mad-sens5</b> | <b>Mad-sens6</b> | <b>Mad-sens7</b> |
|---|------------------|------------------|--|------------------|------------------|------------------|------------------|------------------|
| MSY-RMS   | 123,379          | 105,537          | 107,864                                | 114,673          | 121,037          | 126,395          | 130,515          | 134,010          |
| $B_{\text{MSY}} - B_{\text{RMS}}$                                     | 565,617          | 425,993          | 389,211                                | 406,529          | 416,454          | 421,992          | 424,606          | 426,046          |
| $S_{\text{MSY}} - S_{\text{RMS}}$                                     | 169,233          | 115,829          | 95,101                                 | 97,768           | 97,168           | 96,336           | 94,607           | 92,750           |
| $B_{\text{MSY}}/B_0 - B_{\text{RMS}}/B_0$                             | 0.28             | 0.27             | 0.26                                   | 0.26             | 0.26             | 0.26             | 0.26             | 0.27             |
| $S_{\text{MSY}}/S_0 - S_{\text{RMS}}/S_0$                             | 0.27             | 0.23             | 0.21                                   | 0.21             | 0.2              | 0.2              | 0.2              | 0.2              |
| $C_{\text{recent}}/\text{MSY} - C_{\text{recent}}/\text{RMS}$         | 0.84             | 0.99             | 0.97                                   | 0.91             | 0.86             | 0.82             | 0.8              | 0.78             |
| $B_{\text{recent}}/B_{\text{MSY}} - B_{\text{recent}}/B_{\text{RMS}}$ | 0.31             | 0.58             | 1.00                                   | 1.21             | 1.35             | 1.44             | 1.5              | 1.55             |
| $S_{\text{recent}}/S_{\text{MSY}} - S_{\text{recent}}/S_{\text{RMS}}$ | 0.2              | 0.47             | 0.96                                   | 1.22             | 1.39             | 1.5              | 1.58             | 1.63             |
| <i>F multiplier-</i>  |                  |                  |  |                  |                  |                  |                  |                  |
| Multiplicador de $F$  | 0.4              | 0.64             | 1.05                                   | 1.29             | 1.48             | 1.62             | 1.72             | 1.81             |
| $\lambda = 1$ , all fisheries—<br>todas pesquerías                    | <b>Mad-sens1</b> | <b>Mad-sens2</b> | <b><math>\lambda = 1</math></b>        | <b>Mad-sens3</b> | <b>Mad-sens4</b> | <b>Mad-sens5</b> | <b>Mad-sens6</b> | <b>Mad-sens7</b> |
| MSY-RMS   | 133,834          | 111,103          | 95,544                                 | 100,851          | 102,766          | 108,296          | 115,942          | 122,755          |
| $B_{\text{MSY}} - B_{\text{RMS}}$                                     | 663,082          | 454,769          | 340,276                                | 338,034          | 337,600          | 350,831          | 371,995          | 388,208          |
| $S_{\text{MSY}} - S_{\text{RMS}}$                                     | 205,439          | 126,585          | 82,911                                 | 78,926           | 76,612           | 78,414           | 81,777           | 83,760           |
| $B_{\text{MSY}}/B_0 - B_{\text{RMS}}/B_0$                             | 0.3              | 0.3              | 0.29                                   | 0.29             | 0.29             | 0.28             | 0.28             | 0.28             |
| $S_{\text{MSY}}/S_0 - S_{\text{RMS}}/S_0$                             | 0.3              | 0.26             | 0.23                                   | 0.22             | 0.22             | 0.21             | 0.21             | 0.21             |
| $C_{\text{recent}}/\text{MSY} - C_{\text{recent}}/\text{RMS}$         | 0.78             | 0.94             | 1.09                                   | 1.03             | 1.01             | 0.96             | 0.9              | 0.85             |
| $B_{\text{recent}}/B_{\text{MSY}} - B_{\text{recent}}/B_{\text{RMS}}$ | 0.21             | 0.39             | 0.59                                   | 0.83             | 1.03             | 1.24             | 1.43             | 1.56             |
| $S_{\text{recent}}/S_{\text{MSY}} - S_{\text{recent}}/S_{\text{RMS}}$ | 0.11             | 0.22             | 0.41                                   | 0.59             | 0.8              | 1.02             | 1.22             | 1.36             |
| <i>F multiplier-</i>  |                  |                  |  |                  |                  |                  |                  |                  |
| Multiplicador de $F$  | 0.27             | 0.4              | 0.57                                   | 0.73             | 0.91             | 1.12             | 1.34             | 1.52             |